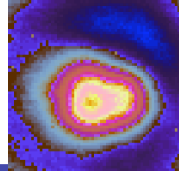


Micro-Models

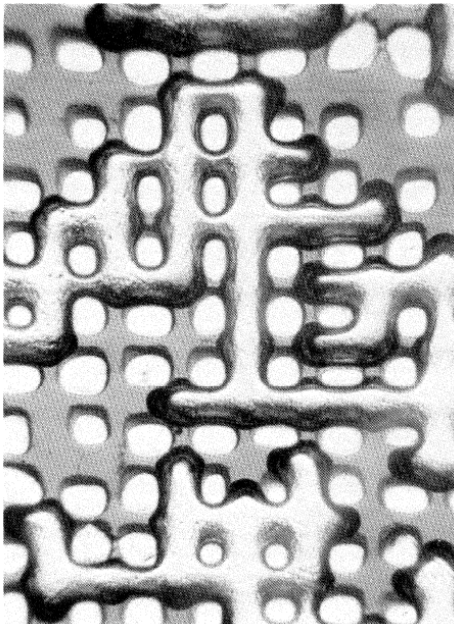


Lecture 1: Fabrication & Image Analysis

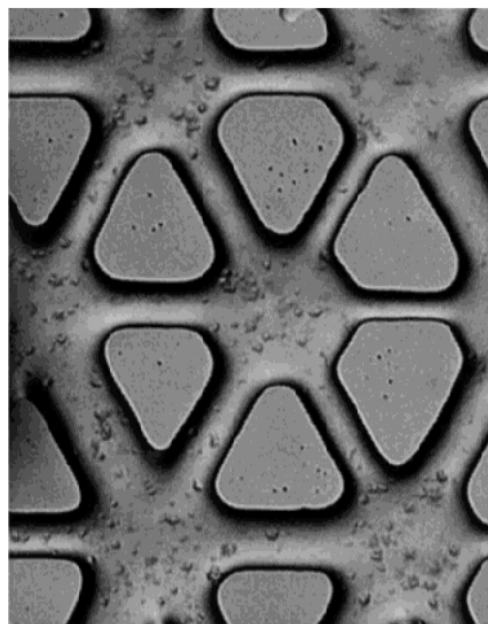
*Laura J. Pyrak-Nolte** ‡

*Department of Physics

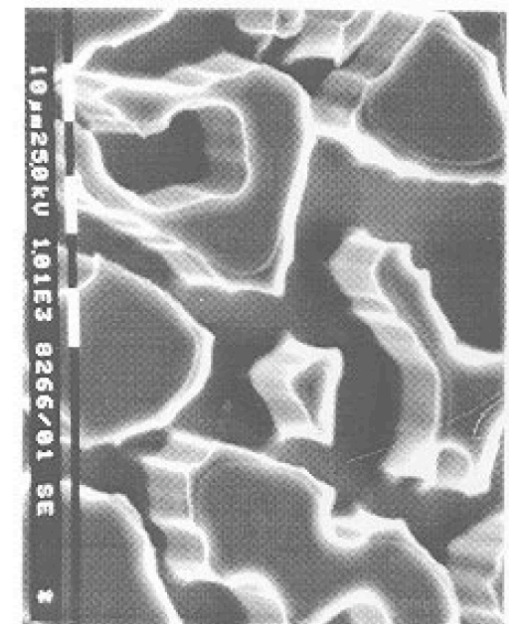
‡ Department of Earth & Atmospheric Sciences
Purdue University



(Lenormand *et al.*, 1983)

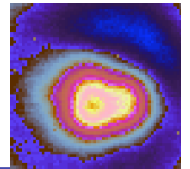


(Stewart & Fogler, 2001)



(Keller *et al.*, 1997)

<http://www.physics.purdue.edu/rockphys/mmliterature.php>



Laboratory for Applied Experimental Geophysics Department of Physics Purdue University

http://www.physics.purdue.edu/rockphys/mmliterature.php

Google

3D particle ...ng using IDL ReversePhone Elijah_Moun...n_Gem_Mine DOE – Fossi...h Programs Request for ... with RPSEA nolte Advanced En...tium: home

Dept. of Physics PHYS 241 ISRM ARMA AGU SEG MatWeb e-Data

PURDUE
UNIVERSITY

Laboratory for Applied
Experimental Geophysics

Department of Physics
Purdue University

[Home](#) | [Wave Propagation](#) | [Fracture Geometry](#) | [Fluid Flow](#) | [Porous Media](#) | [Food](#)

Literature Related to Micro-Model Lectures given on July 20, 2009 by Prof. [Laura J. Pyrak-Nolte](#) at the Summer School on

"[Role of Interfacial Area in Two-Phase Flow and Transport in Porous Media: Theory, Experiment, Modeling](#)"

in Utrecht, Netherlands 19-24 July 2009.

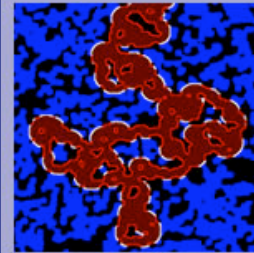
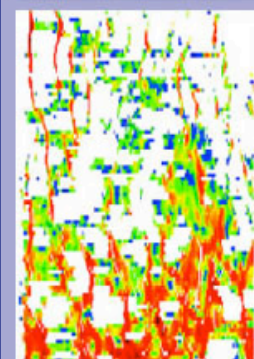
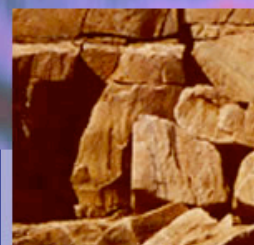
Glass Beads & Glass Shards

Chatenever, A. and J. C. Calhoun, Jr., [Visual examinations of fluid behavior in porous media - Part 1](#), Petroleum Transaction, AIME, vol 195, T.P. 3310, 149-156, 1952

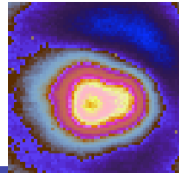
Fourar, M., Bories, S., Lenormand, R. & P. Persoff, [Two-Phase Flow in Smooth and Rough Fractures' Measurement and Correlation by Porous-Medium and Pipe Flow Models](#), WATER RESOURCES RESEARCH, VOL. 29, NO. 11, PAGES 3699-3708, NOVEMBER 1993

Montemagno, C. D. and W. G. Gray, [Photoluminescent volumetric imaging: A technique for the exploration of multiphase flow and transport in porous media](#), GEOPHYSICAL RESEARCH LETTERS, VOL. 22, b10, 4, PAGES 425-428, FEBRUARY 15, 1995

Pyrak-Nolte



Outline



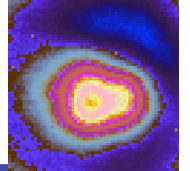
*What is a micro-model?

*Fabrication & Examples

*Imaging Modalities

*Image Analysis

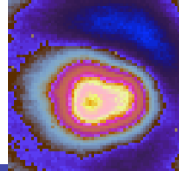
What is a micro-model?



*A transparent flow cell that enables direct visualization of fluid motion, chemical reactions, biological behavior and other processes

Why use micro-models?

*To test theoretical hypotheses on the relationships among capillary pressure, saturation and interfacial area per volume...and other things



Micro-Model Applications

Table 1. Selected applications of micromodels.

Class	Objective	Micromodel	Pore structure	Reference
Microbiology	Dispersion of <i>E. coli</i> Growth and mobility of biofilms	glass	homogen., cylinder homogen., triangular network cubic channel with heterog. apertures	Lanning and Ford (2002) Stewart and Fogler (2002, 2001), Kim and Fogler (2000) Dupin and McCarty (2000), Nambi et al. (2003)
Multiphase processes	Dissolution of NAPLs, determination of mass transfer rates	glass	homogen., tubes	Sahloul et al. (2002), Jia et al. (1999), Zhong et al. (2001)
	Transport of NAPLs in unsat. porous media	glass	monolayer of glass beads	Kennedy and Lennox (1997)
	Soil cleanup with surfactants	silicon wafer	homogen., heterogen.	Chomsurin and Werth (2003)
	Numerical modeling of three-phase flow	silicon water	pore structure taken from a thin section of sand stone	Keller et al. (1997)
	Fluid flow	glass	homogen. cubic network, heterogen. network	Jeong et al. (2000)
		glass	homogen. network	Pereira et al. (1996), Pereira (1999)
	Capillary rise	glass	monolayer of glass beads	Corapcioglu and Fedirchuk (1999)
	Development of air bubbles	glass	homogen. network	Corapcioglu et al. (1997), Soll et al. (1993)
	Fracture-matrix interactions	glass	triangular network	Bernadiner (1998)
Oil exploration	Cementation due to gas hydrates	glass	homogen. pore network with fracture	Li and Yortsos (1995)
	Kinetics of carbonate cementation in wells	glass		Haghghi et al. (1994), Wan et al. (1996)
	Effects of injected polymer gels on the flow of water and oil	glass		Tohidi et al. (2001)
	Transport of gas condensate	glass		Dawe and Zhang (1997)
		glass		Al-Sharji et al. (2001)
Colloids	Attachment at the air-water-interface	glass	homogen., heterogen.	Jamiolahmady et al. (2000), Coskuner (1997), Wang and Mohanty (2000), Bora et al. (2000)
		glass		Wan and Wilson (1994b), Wan et al. (1996)

(from Baumann & Werth, 2004)

Pyra&Nolte

Micro-Model Applications

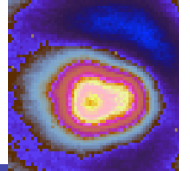
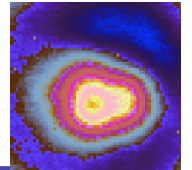


Table 2. Selected Applications of Micromodels for Visualization of Colloidal Transport in Porous Media

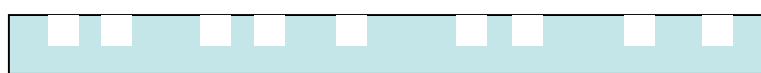
Source	Type of Micromodel	Network Characteristics	Pore Dimensions, μm	Visualization Method	Moisture Conditions	Nature of Colloids (Size, μm)	Objective
Wan and Wilson [1994]	etched glass	regular polygon pillars and irregular shapes	200 ^a /50 ^b ; 300 ^a /20–100 ^b ; 4–400	dark-field; epifluorescence	unsaturated	hydrophilic microspheres (0.6, 1.05); hydrophobic microsphere (0.95); bacteria (1.2×0.8 , 1.0×0.8); clay (0.5)	attachment at the air-water interface
Wan et al. [1996] Lanning and Ford [2002]	etched glass etched glass	two-domain: fracture-matrix regular cylindrical pillars	range of widths 0–600 ^c 360–375 \times 60–83 ^c	epifluorescence light scattering to determine turbidity	saturated saturated	microspheres (1.0) <i>E. coli</i>	two-domain flow dispersion of bacteria
Sirivithayapakorn and Keller [2003a]	etched silicon	simulation of natural pore system	2.4 – 30 \times 15 ^c	epifluorescence	saturated	latex microspheres (0.05, 1.0, 2.0, 3.0); stained bacteriophage	size exclusion and colloid acceleration
Sirivithayapakorn and Keller [2003b]	etched silicon	simulation of natural pore system	2.4 – 30 \times 15 ^c	epifluorescence	unsaturated	latex microspheres (0.05, 1.0, 2.0, 3.0); stained bacteriophage	dissolution of air-water interface
Auset and Keller [2004]	molded silicon (PDMS ^d)	rounded square pillars	10, 20 \times 12 ^c	epifluorescence	saturated	latex microspheres (2,3,5,7)	colloid dispersion
Baumann and Werth [2004]	etched silicon	regular cylindrical pillars	173 ^a /35 ^b \times 50 ^c	epifluorescence	saturated	microspheres (0.691,1.96)	comparison to LB model and filtration theory predictions ^e
Auset et al. [2005]	molded silicon (PDMS ^d)	simulation of natural pore system	2.4 – 30 \times 12 ^c	epifluorescence	cyclical infiltration and draining	DAPI stained bacteria (2 \times 1); latex microspheres (5)	Intermittent filtration of bacteria and colloids
Chen and Flury [2005]	etched glass	regular cylindrical pillars	70	bright field	unsaturated	natural colloids(0.348), modified colloids (0.368), kaolinite (0.332), Na-montmorillonite (0.324)	retention of mineral colloid in unsaturated media

(from Ochiai et al., 2006)

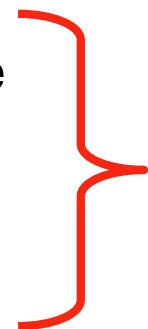
What is a micro-model?



*a transparent flow cell that enables direct visualization of fluid motion, chemical reactions, biological behavior and other processes

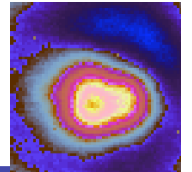


Etched substrate
Etched polymer
Mold
Replicas



Optical or X-ray Lithography

Photoresist



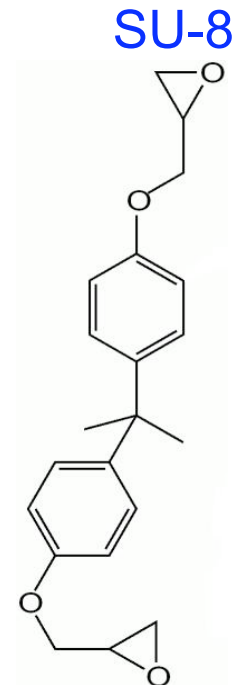
Photoresist: A light sensitive material

PMMA: Polymethylmethacrylate

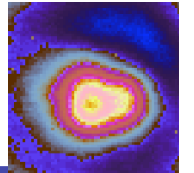
PMGI: PolyMethylGlutarimide

Novolac: phenol formaldehyde resin (PF)

SU-8: epoxy that is a multifunctional glycidyl ether derivate of bisphenol-A novolac. Dissolves in gamma butyrolactone (GBL) to change viscosity & affect film thickness

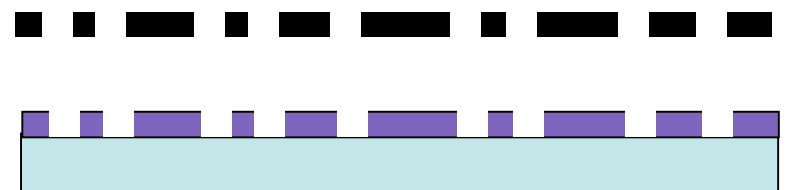


Photoresist



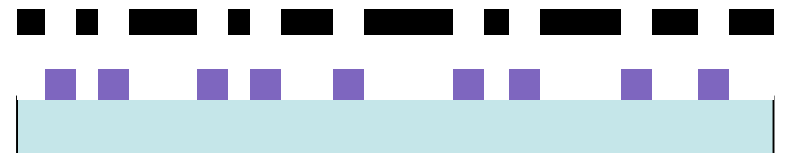
Positive Resist: Regions exposed to UV are washed away upon development.

ex. Shipley 1805 (now Ross & Hass)

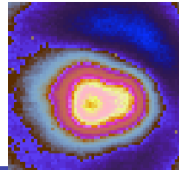


Negative Resist: Regions exposed to UV remain after development

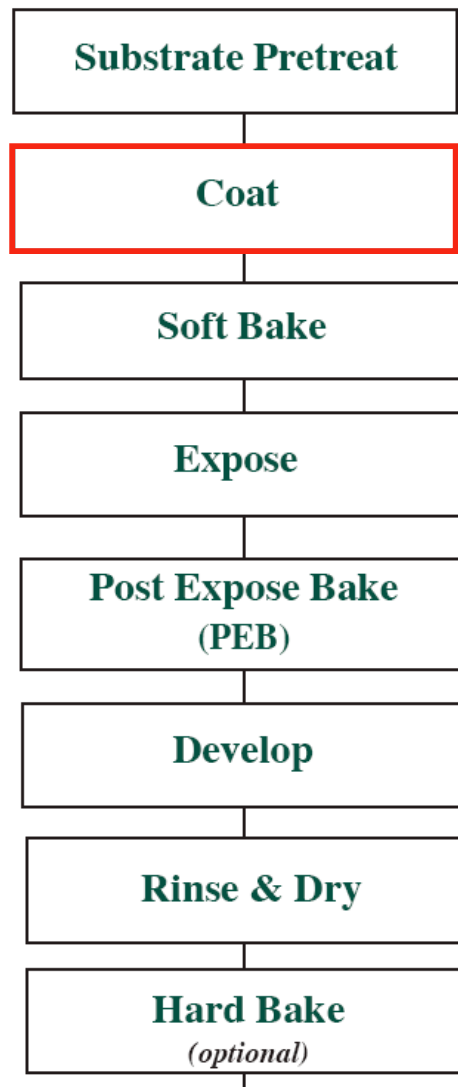
ex. SU-8



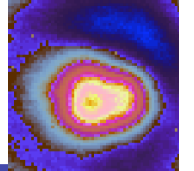
Processing Photoresist



SU-8 Processing Steps

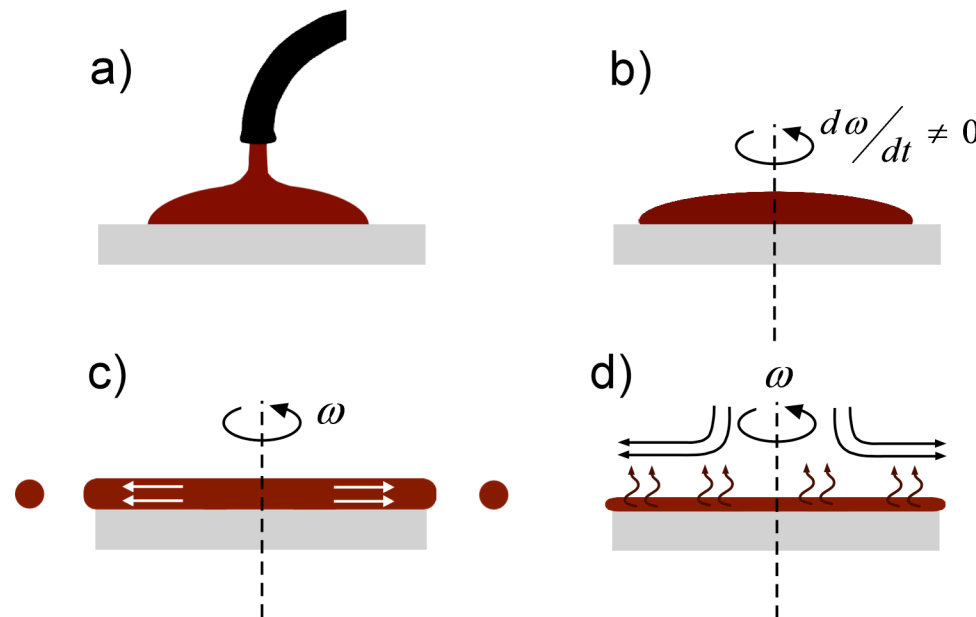


Optical Lithography: Preparation

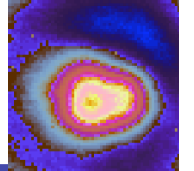


*analogous to darkroom development of photographs

Spin Coating of Disk with a UV-sensitive Polymer

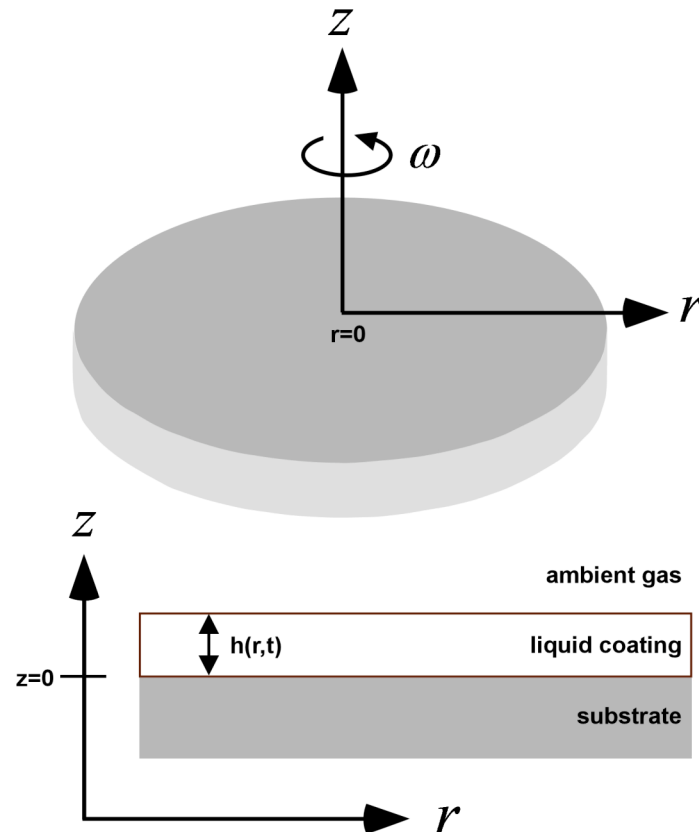


<http://large.stanford.edu/courses/ph210/hellstrom1/>

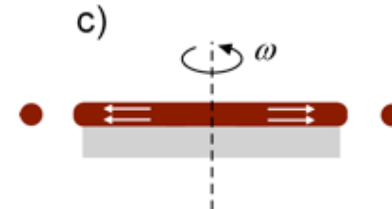


Optical Lithography: Preparation

*analogous to darkroom development of photographs



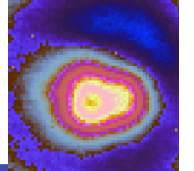
Assuming No Evaporation



$$h = \frac{h_o}{\sqrt{1 + \frac{4\omega^2 \rho h_o^2 t}{3\eta}}}$$

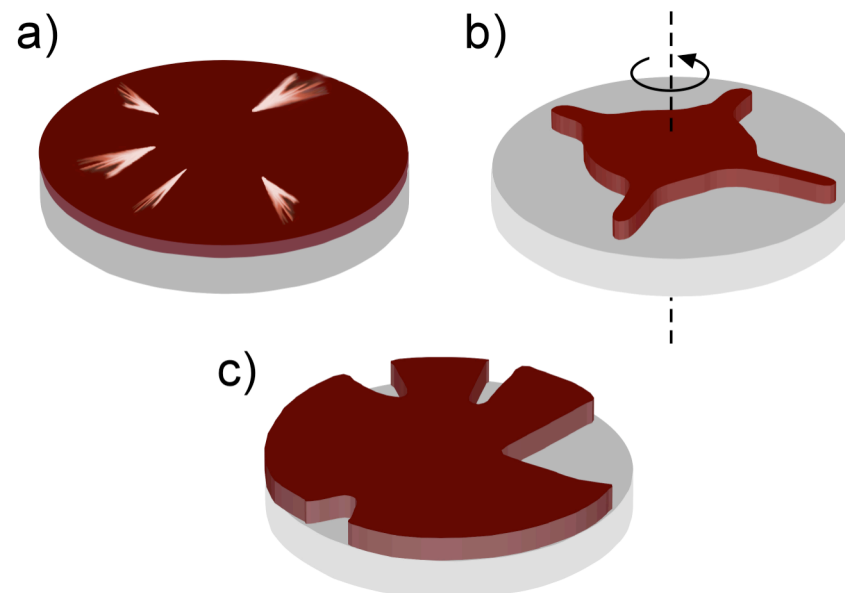
$$r = r_o^{3/4} \sqrt{1 + \frac{4\omega^2 \rho h_o^2 t}{3\eta}}$$

<http://large.stanford.edu/courses/ph210/hellstrom1/>

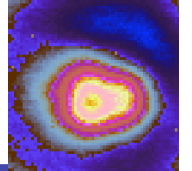


Optical Lithography: Preparation

*Care in spin coating

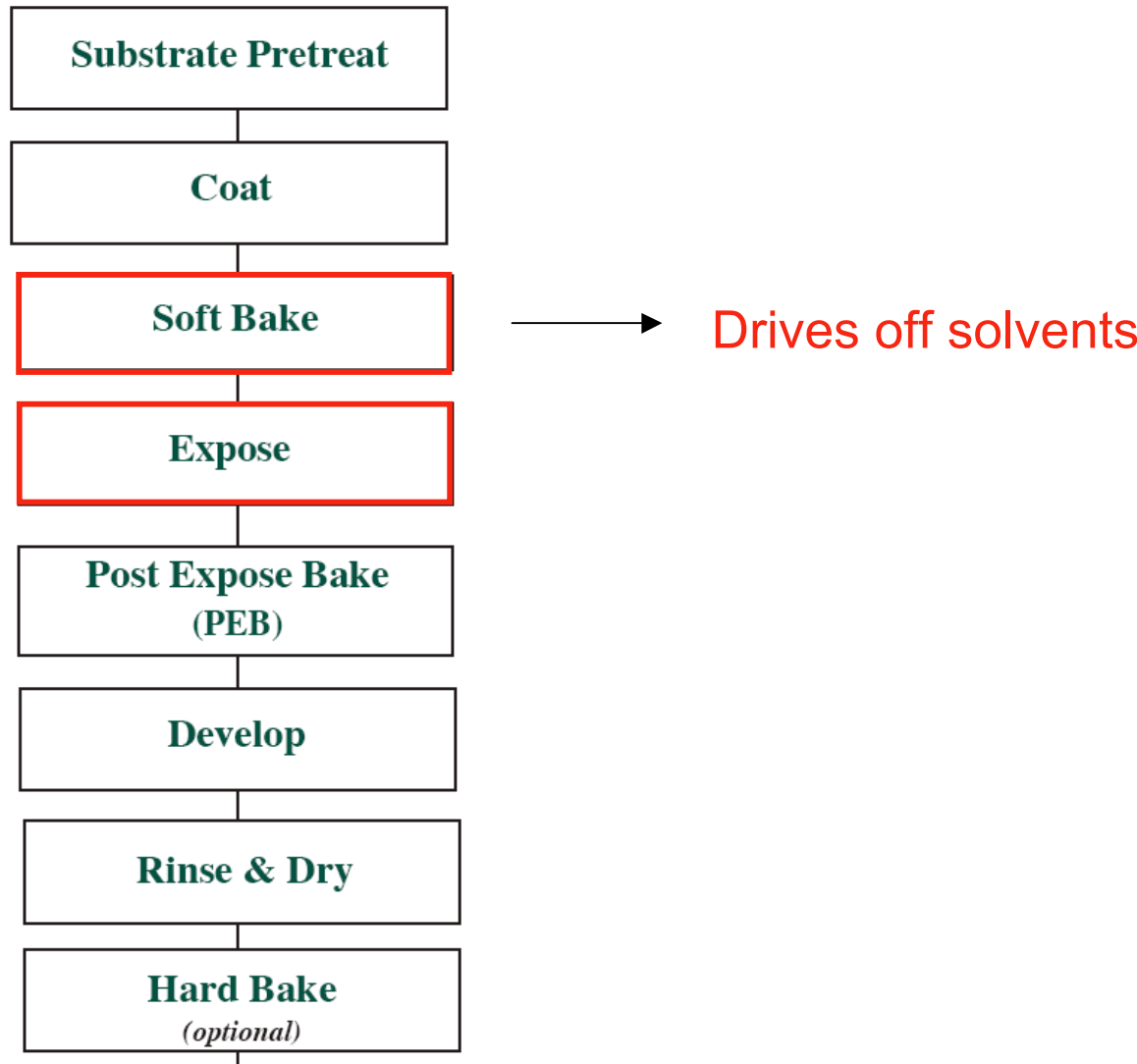


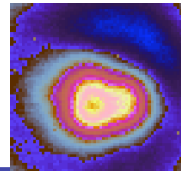
<http://large.stanford.edu/courses/ph210/hellstrom1/>



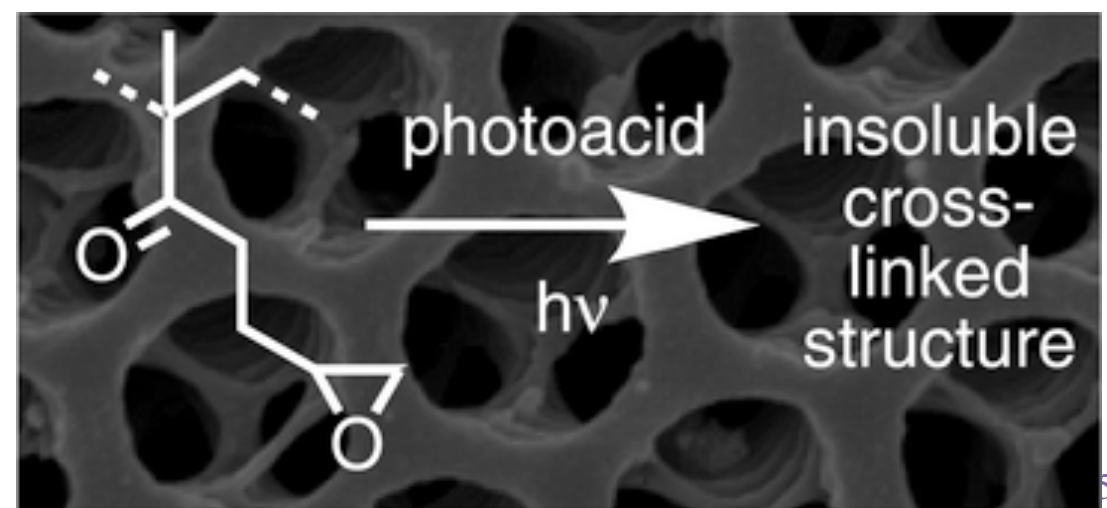
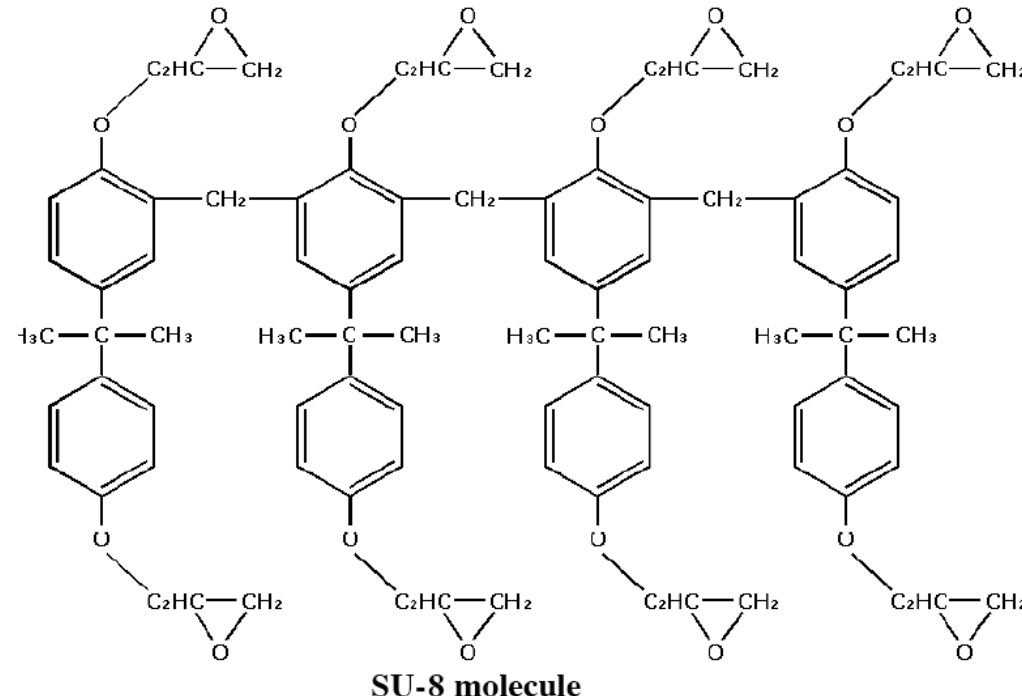
Processing Photoresist

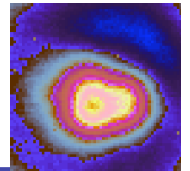
SU-8 Processing Steps



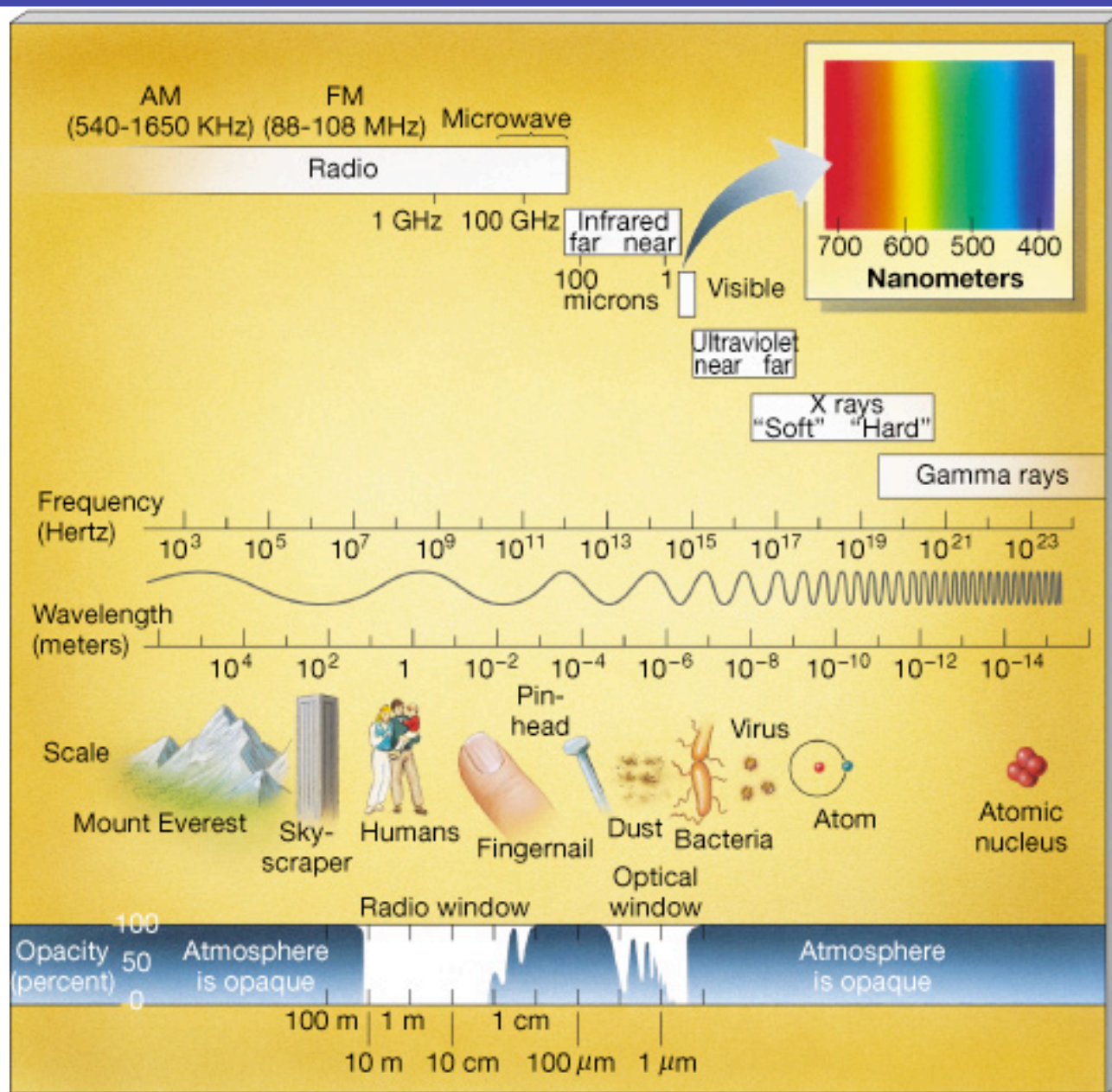


Photolithography: Exposure Induced Cross-linking

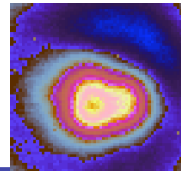




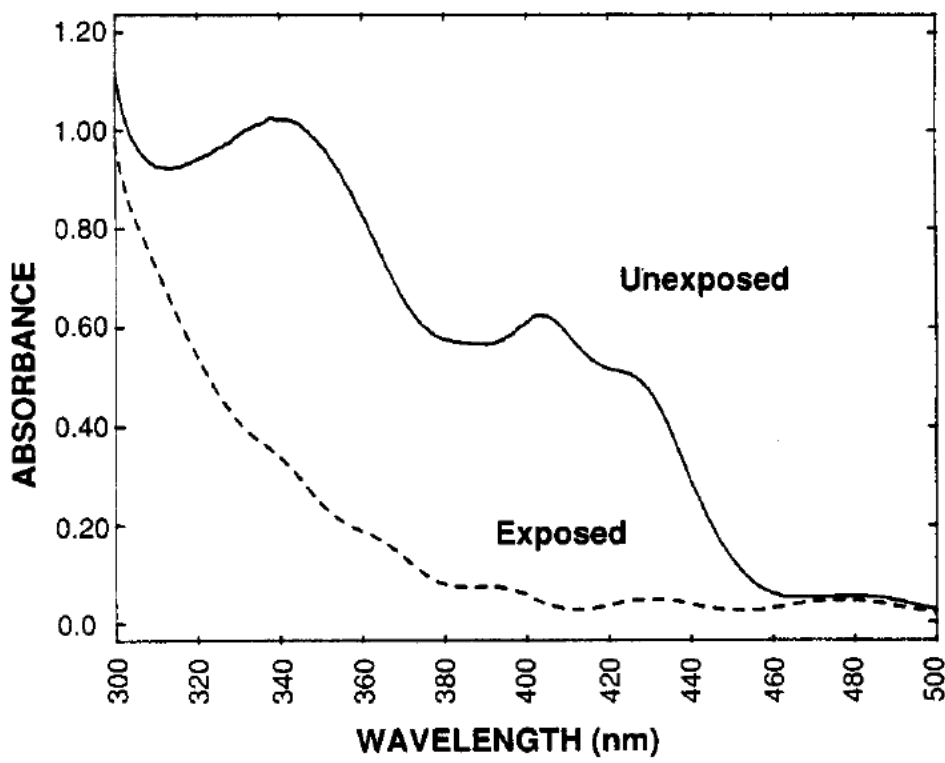
Photolithography: Electromagnetic Spectrum



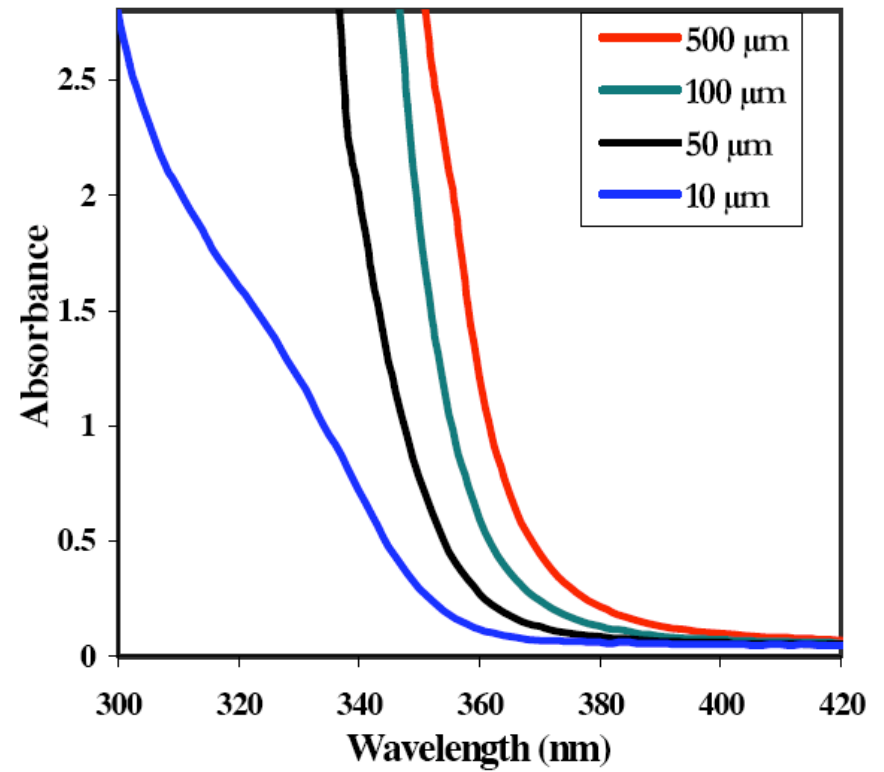
Photolithography: Wavelength for Exposure



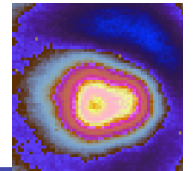
Shipley 1813



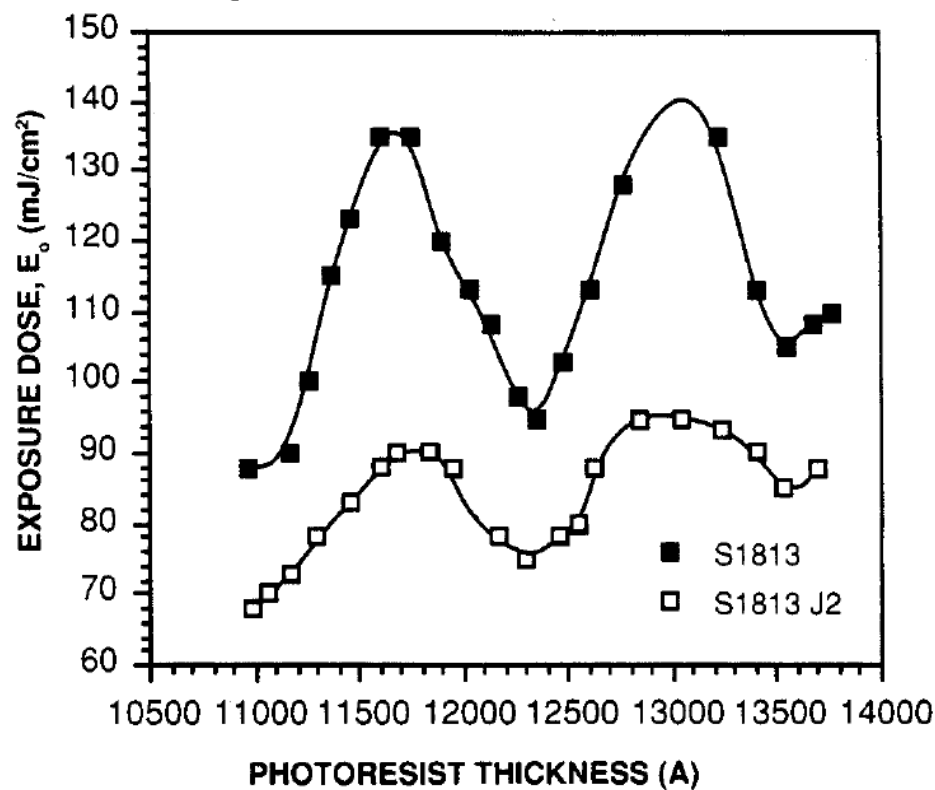
SU-8



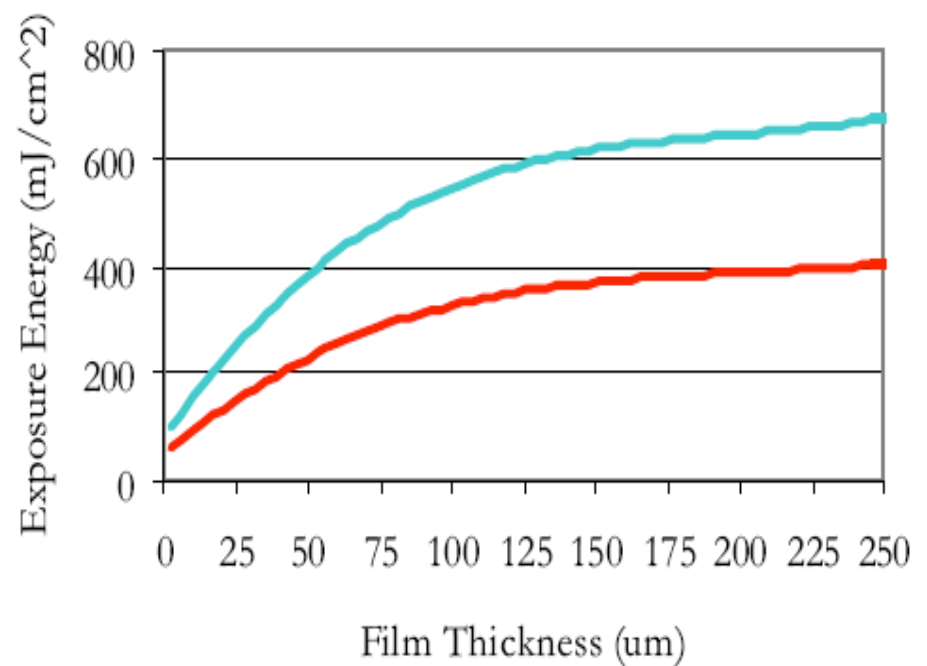
Optical Lithography: Energy Dose for Exposure

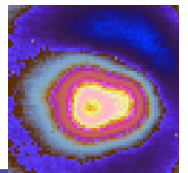


Shipley 1813

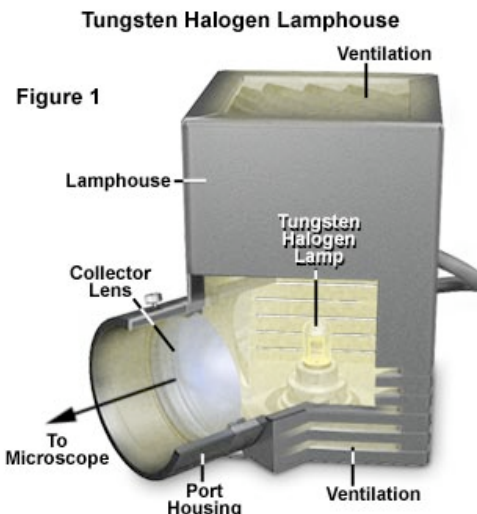


SU-8

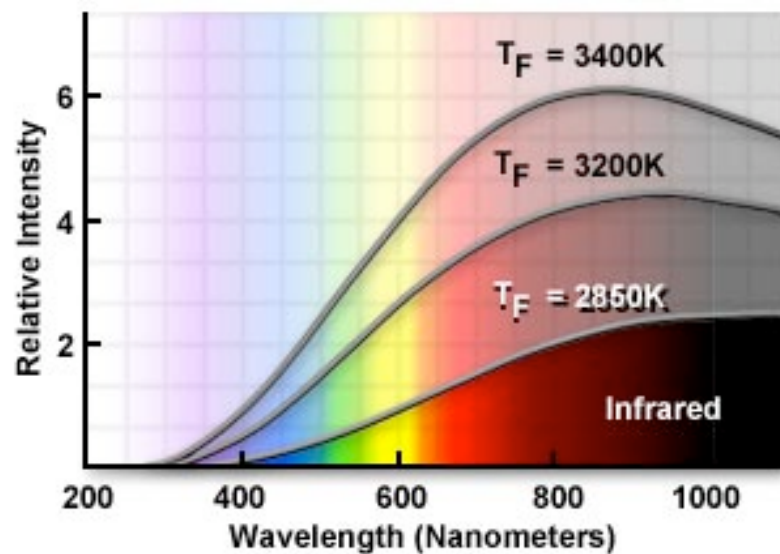




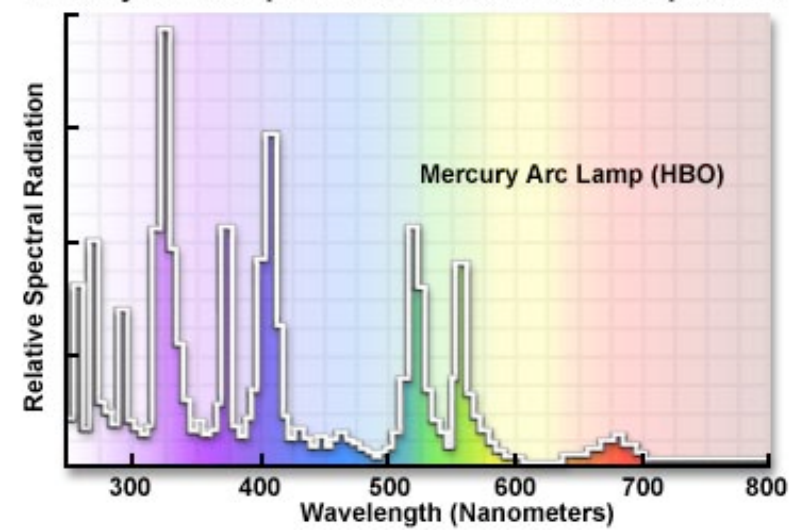
Optical Lithography: Typical Sources



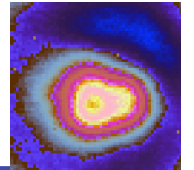
Tungsten Lamp Emission Spectrum



Mercury Arc Lamp UV and Visible Emission Spectrum

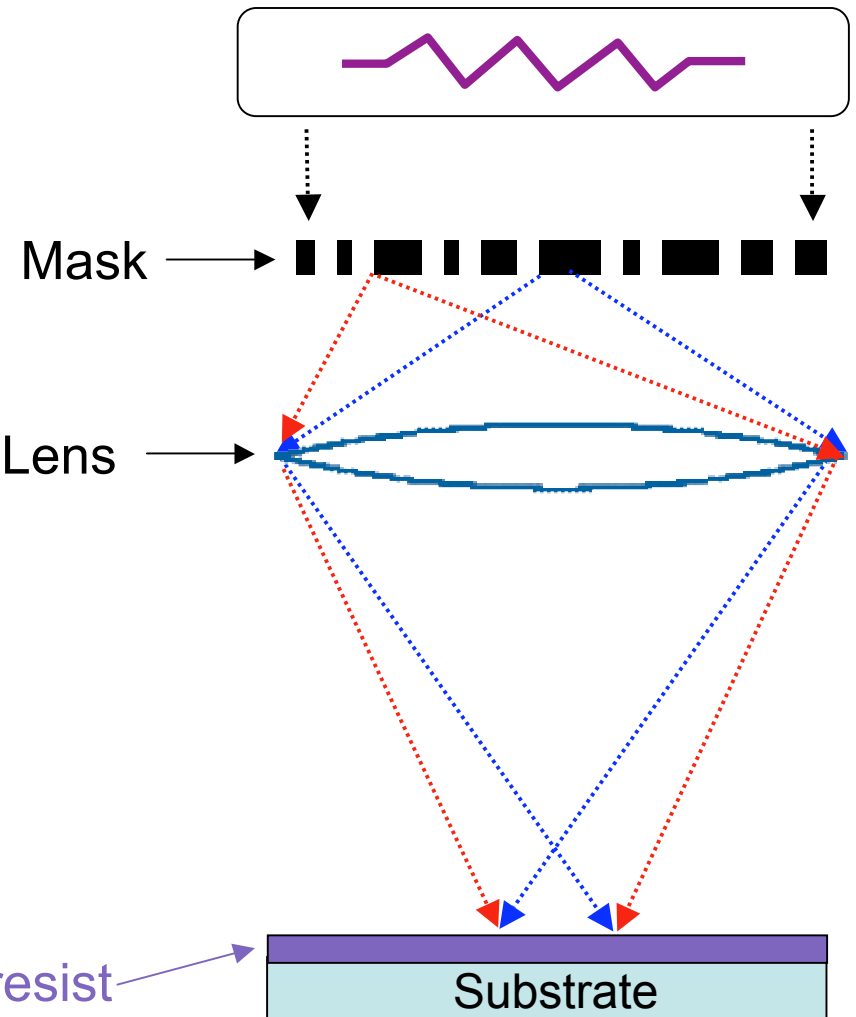


Optical Lithography: Methods



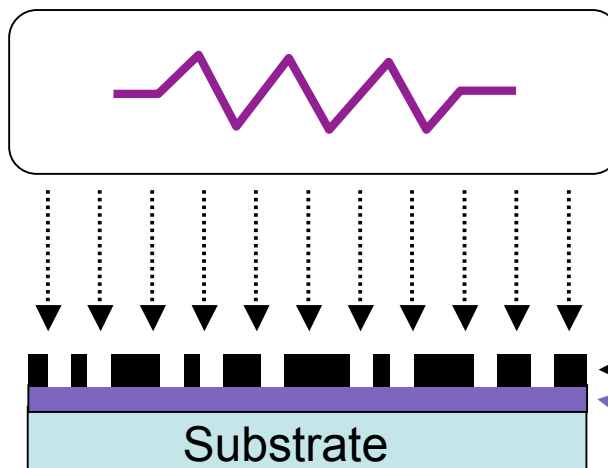
Projection Lithography

Tungsten Light Source

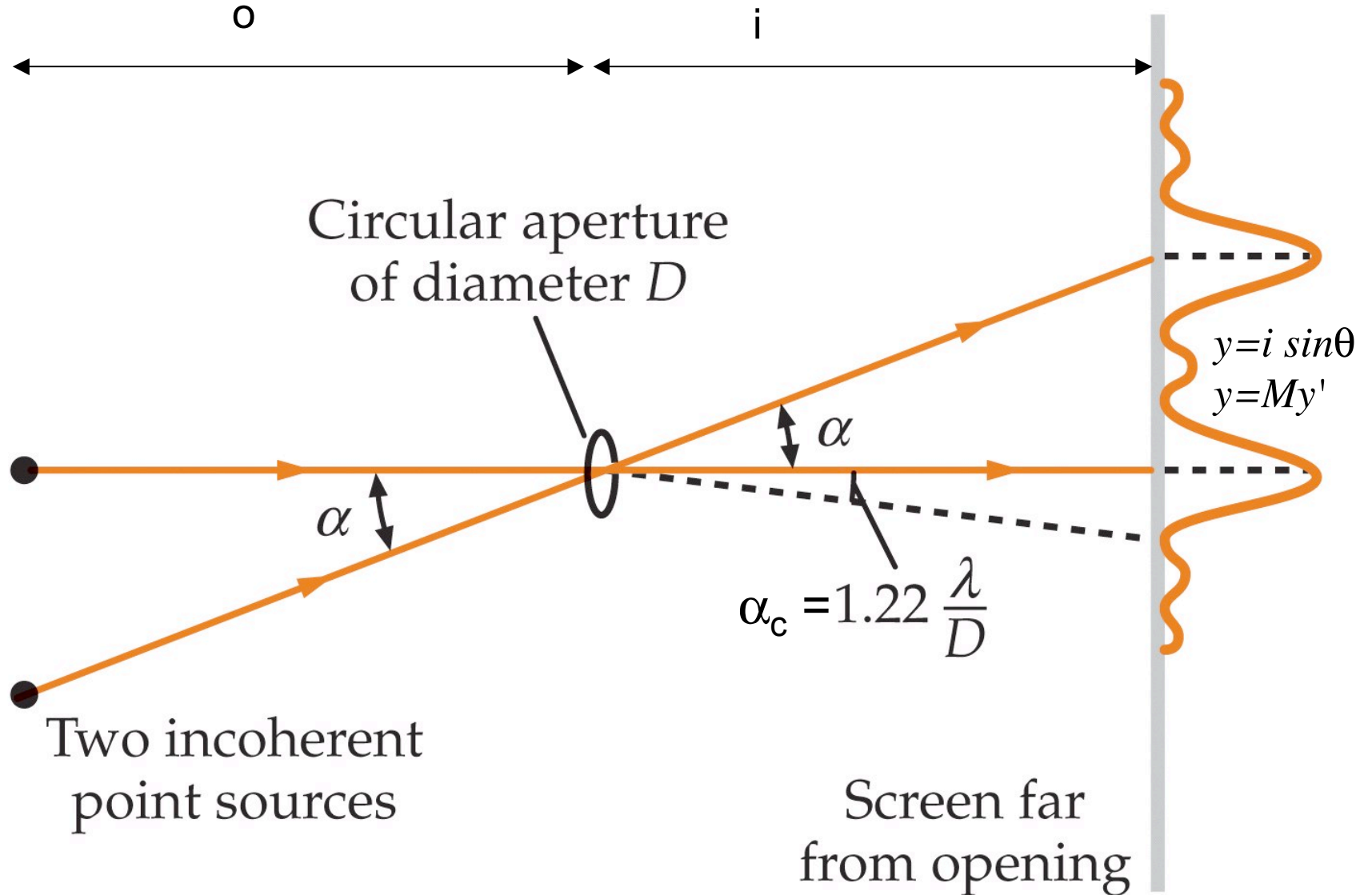
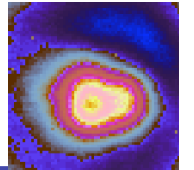


Contact Lithography

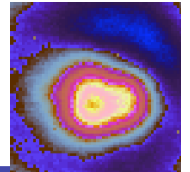
Mercury Light Source



Rayleigh Criteria



Rayleigh Criteria



If $\alpha > \alpha_C$ objects can be resolved

If $\alpha < \alpha_R$ objects can not be resolved

To increase our ability to distinguish objects we must minimize the diffraction pattern. Because

$$\alpha_C \approx 1.22 \frac{\lambda}{d}$$

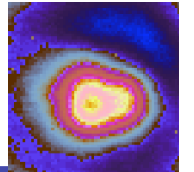
we can :

increase d or

decrease λ

- 1) Use ultraviolet light
- 2) e- beam used in Scanning Electron Microscopes (SEM) have $\lambda \approx \lambda(\text{light})/10^5$
- 3) place object under a microscope in a drop of oil $\lambda_n = \lambda/n$

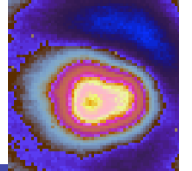
Processing Photoresist



SU-8 Processing Steps

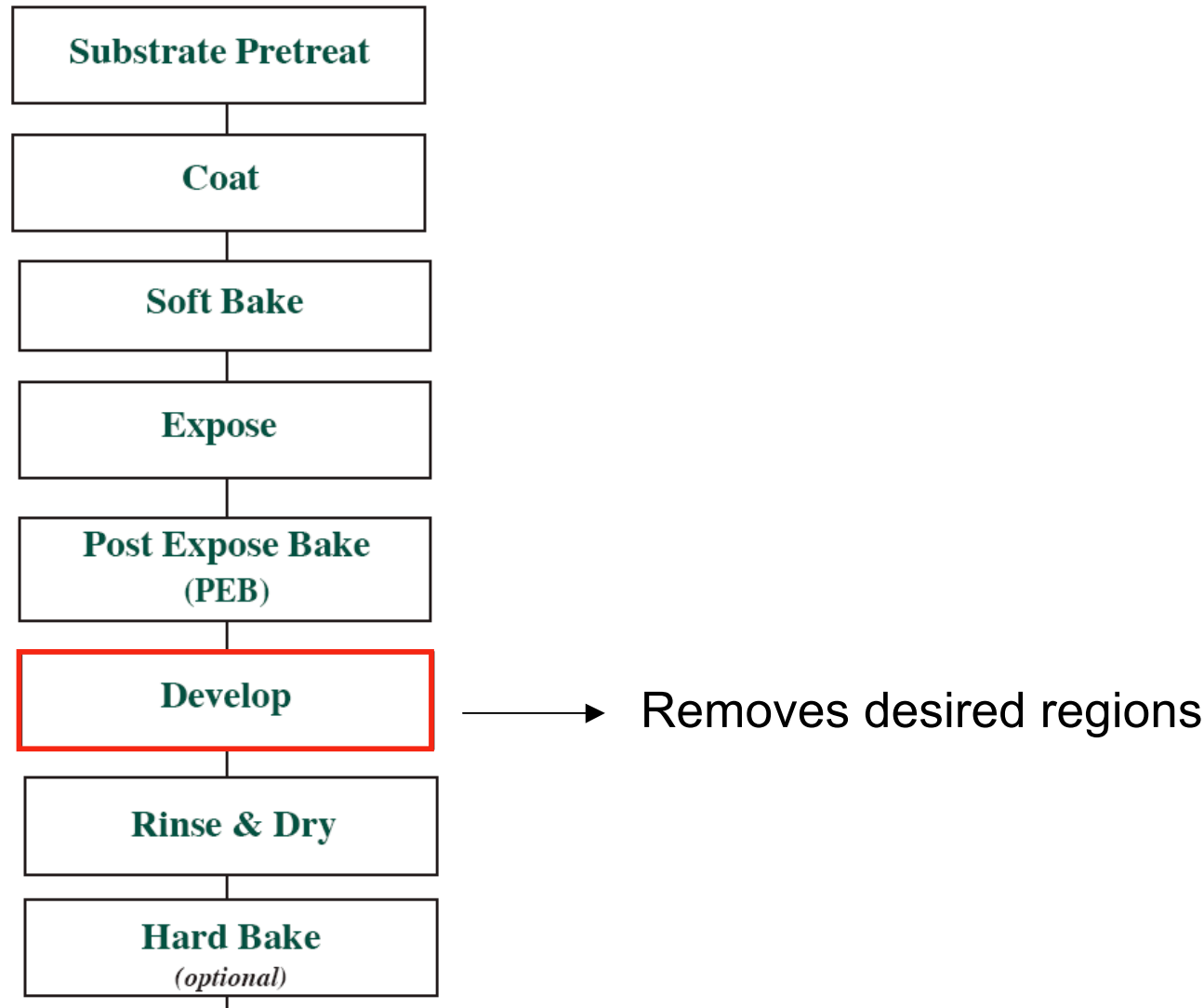


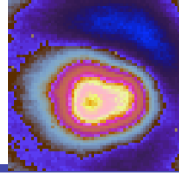
for chemically amplified resists:
catalytically performs and completes
the photo reaction initiated during
exposure. For negative resists,
crosslink during PEB and remain after
development



Processing Photoresist

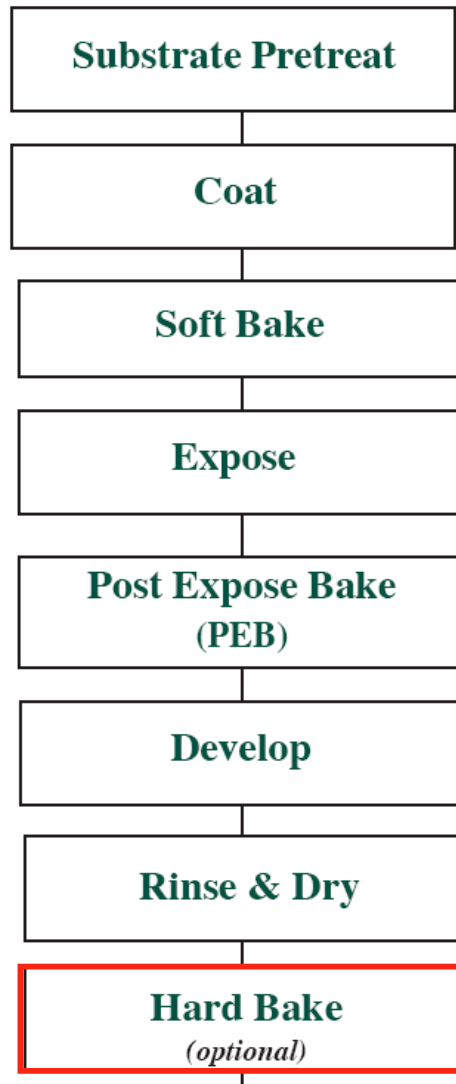
SU-8 Processing Steps



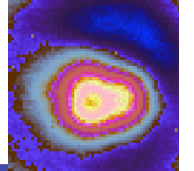


Processing Photoresist

SU-8 Processing Steps

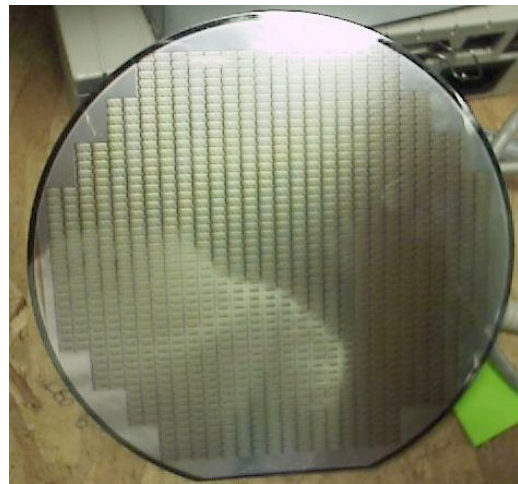


Increases thermal, chemical and physical stability of the structure



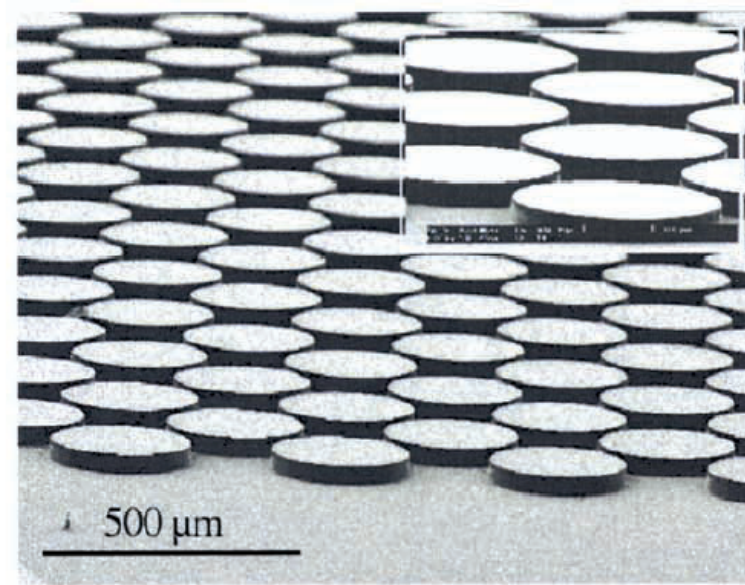
Types of Micro-Models: Etched Silicon or Glass

Silicon Wafer

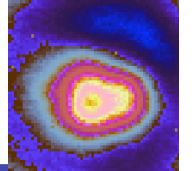


[http://www.computermuseum.li/
Testpage/SiliconWaferofChips.j
pg](http://www.computermuseum.li/Testpage/SiliconWaferofChips.jpg)

Baumann & Werth, 2004



Types of Micro-Models: Etched Silicon or Glass



Baumann & Werth, 2004

440

VADOSE ZONE J., VOL. 3, MAY 2004

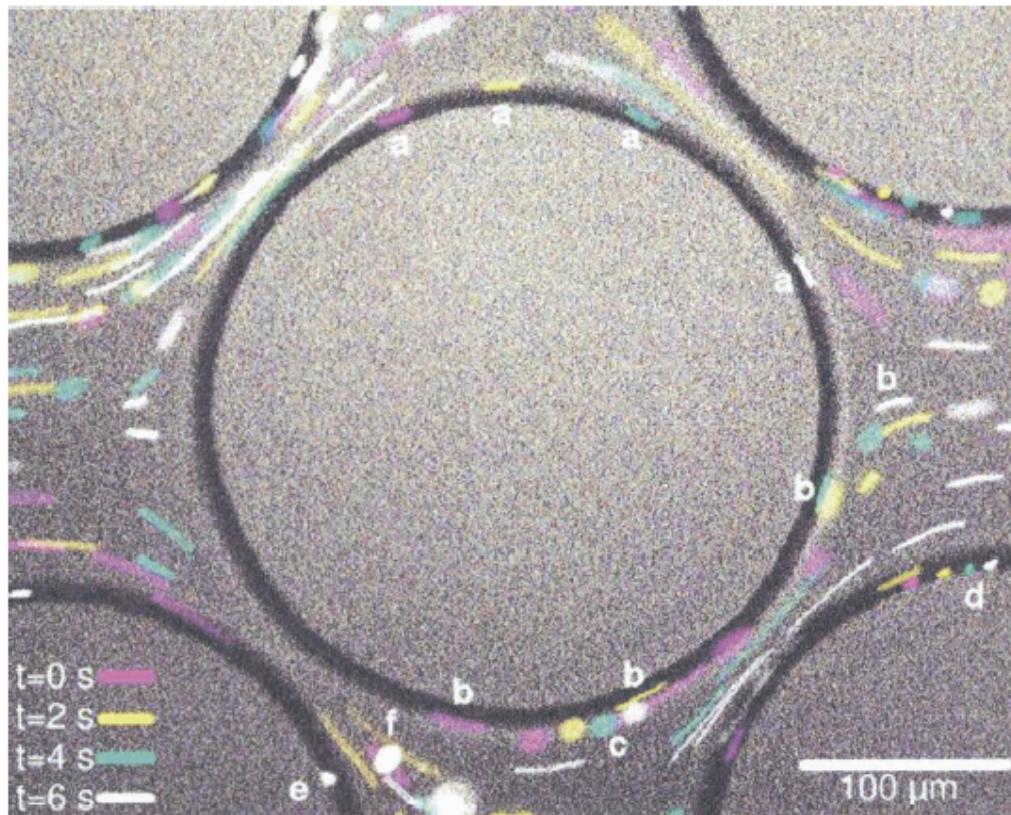
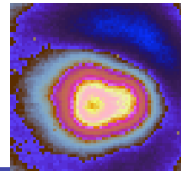
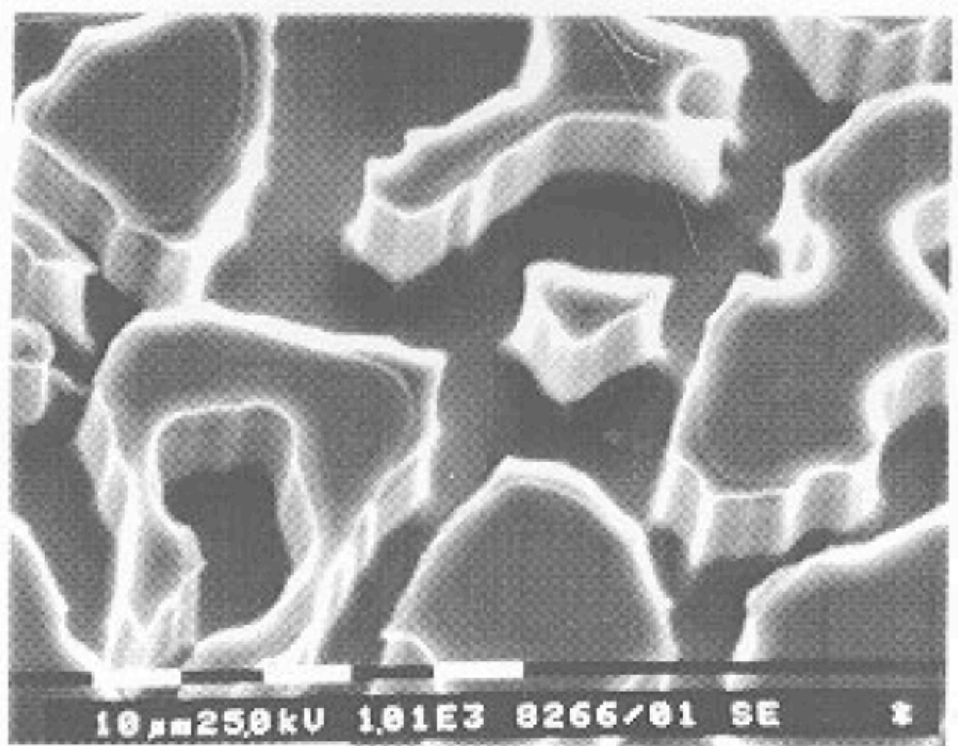
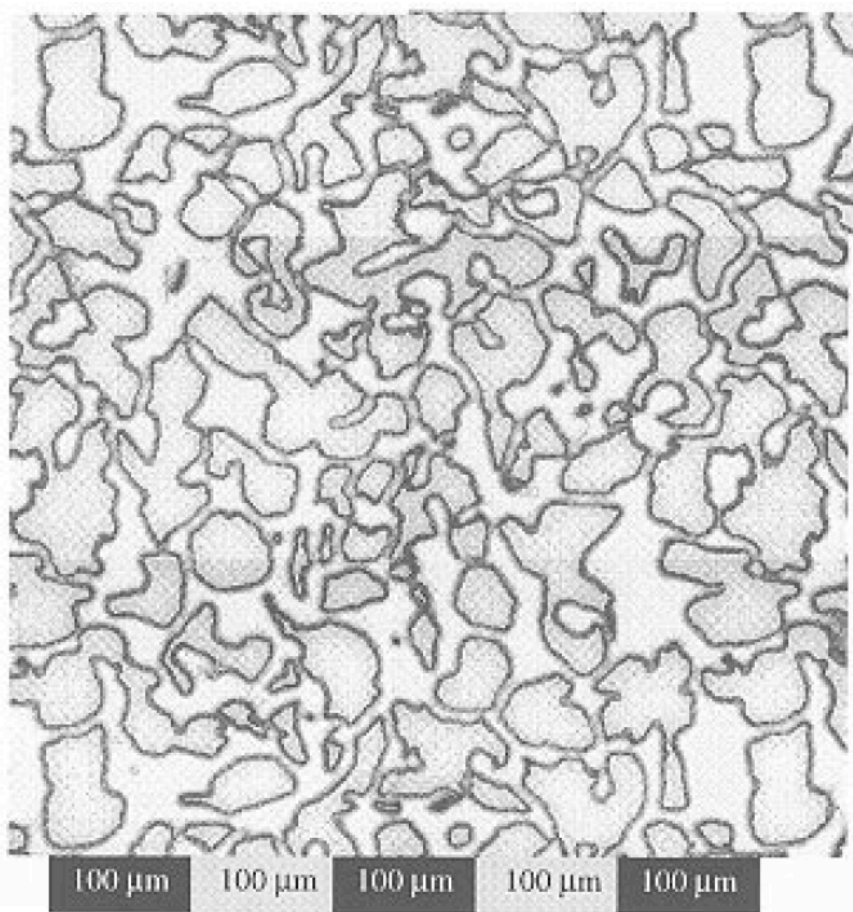


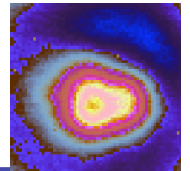
Fig. 4. A composite order image of 691-nm colloids in the homogeneous micromodel. Flow is from left to right at $15 \mu\text{L h}^{-1}$. The color code indicates the position of the colloids at time steps 2 s apart.

Types of Micro-Models: Etched Silicon or Glass



Keller et al., 1997





Types of Micro-Models: Etched Silicon or Glass

Keller et al., 1997

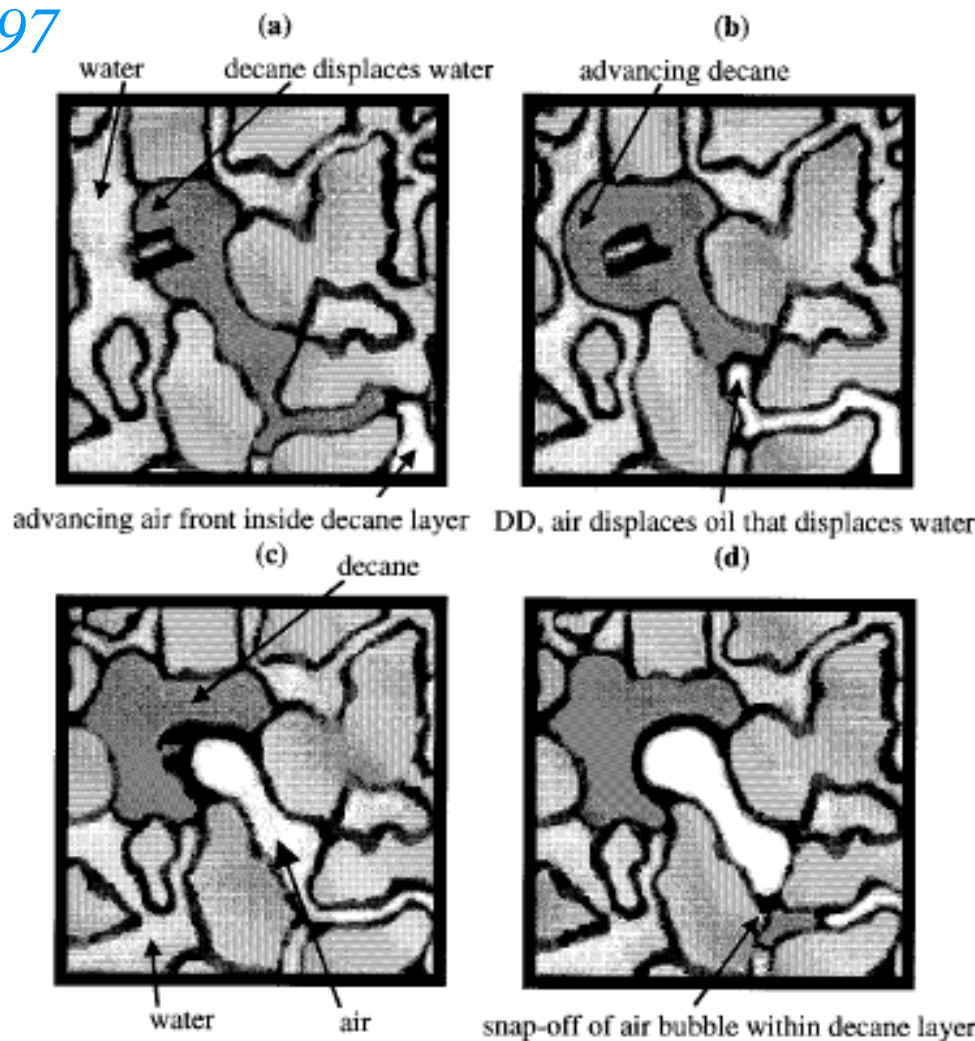
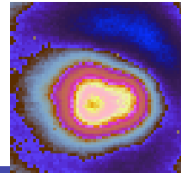
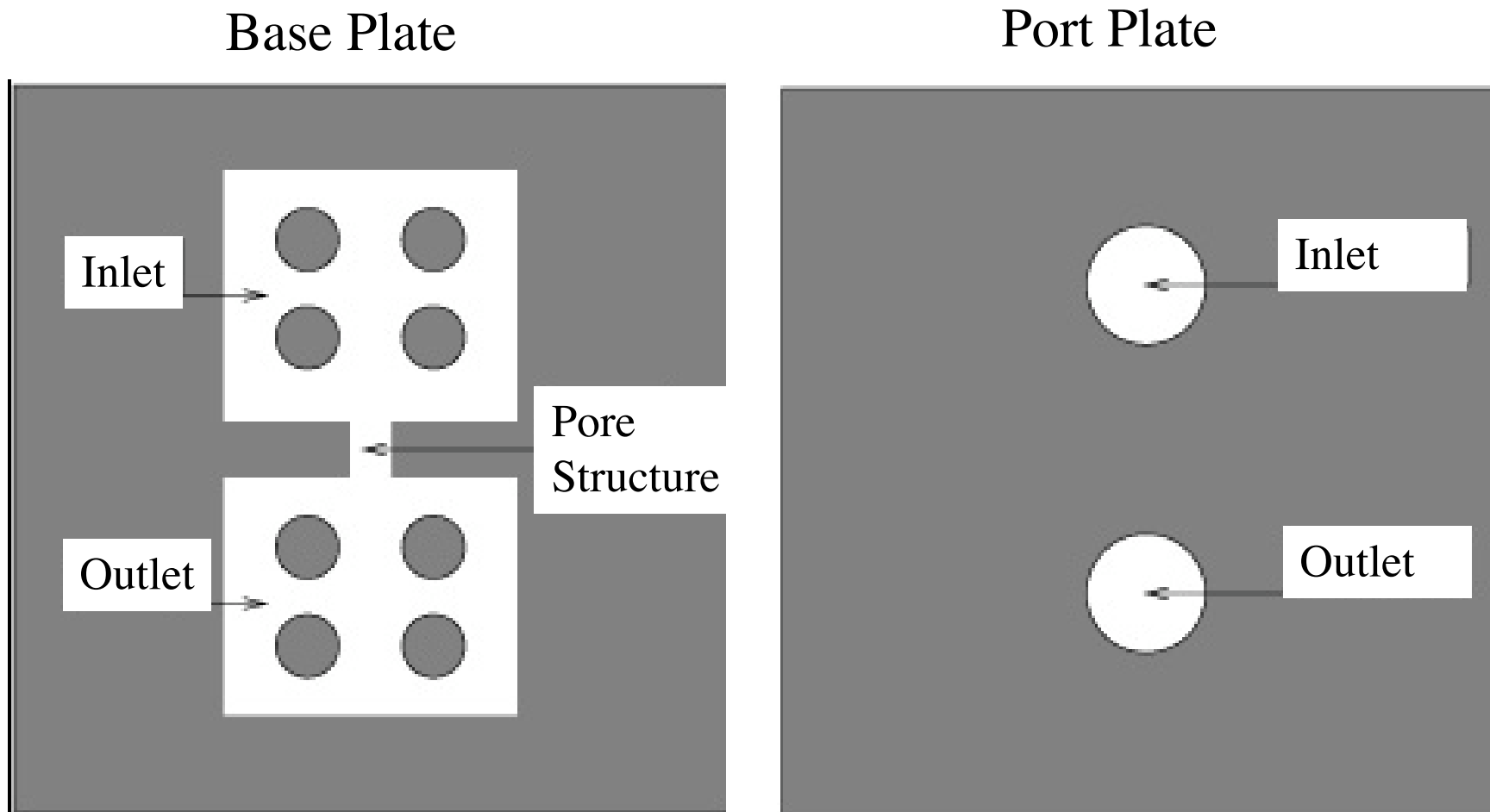


Figure 11. Double drainage sequence, with air displacing decane that displaces water, at the advancing water/decane interface: (a) air surrounded by decane, (b) as the air advances, decane is also forced into the surrounding water – this is double drainage, (c) air displaces decane, (d) snap-off of air front, leaving a disconnected bubble.

Type of Micro-Model: Projection Lithography



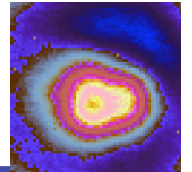
1. Contact Lithography



Cheng et al., 2004

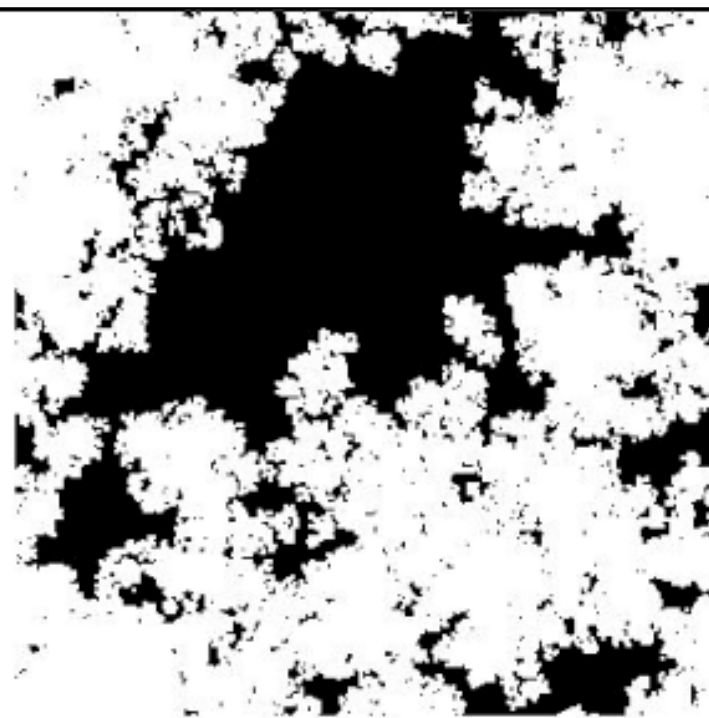
Pyrak-Nolte

Type of Micro-Model: Projection Lithography

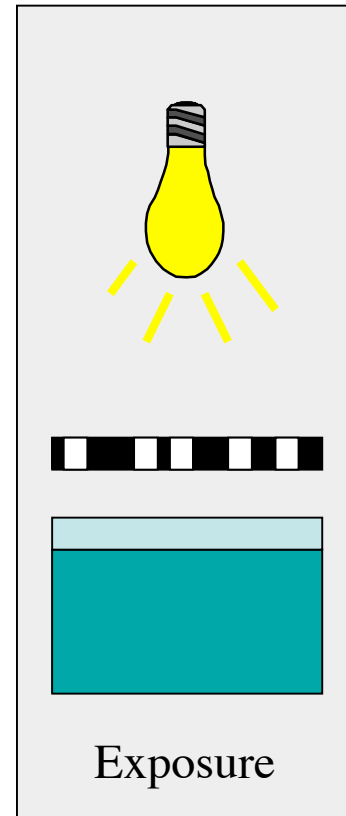


2. Projection Lithography

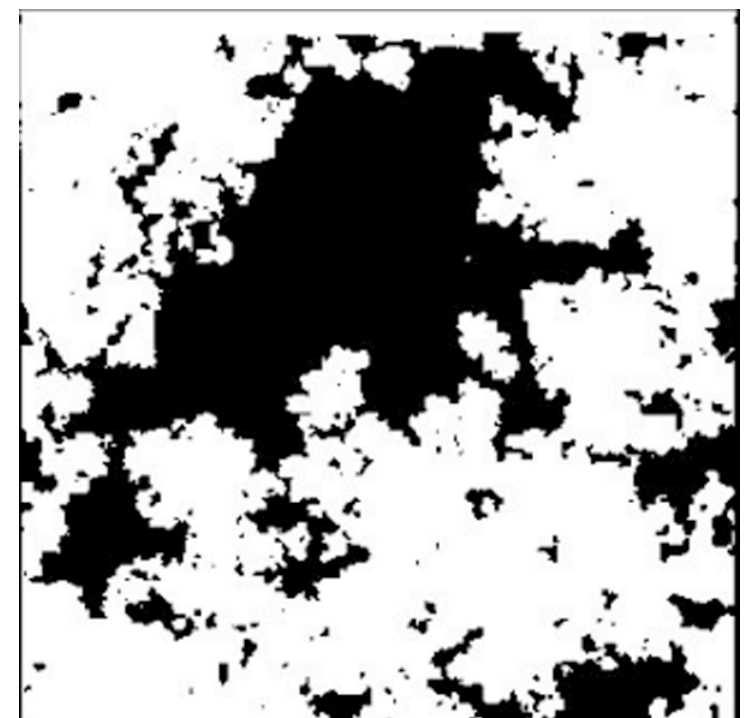
Desired Pattern



Exposure
to UV



After Development
Photoresist Micro-model

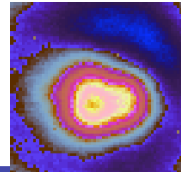


■ - Photoresist

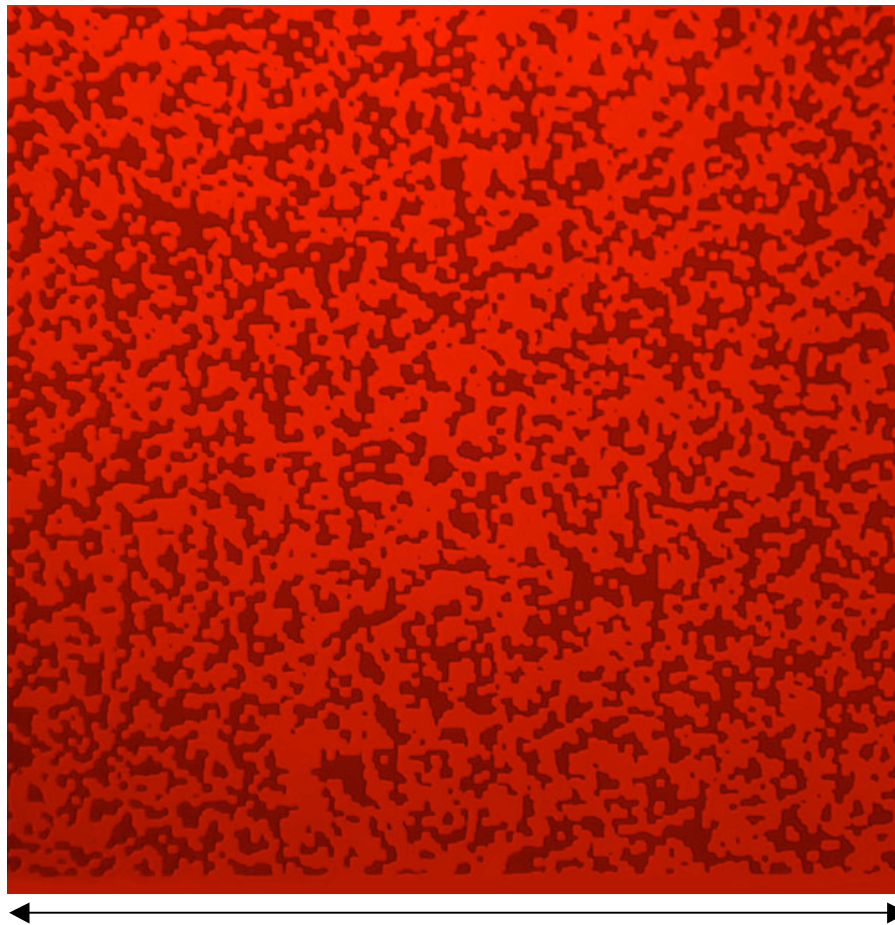
■ - Glass Slide

■ - Mask

Type of Micro-Model: Projection Lithography



Spatially Uncorrelated



600 μm

Cheng et al., 2004

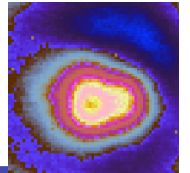
Pyrak-Nolte

Spatially Correlated

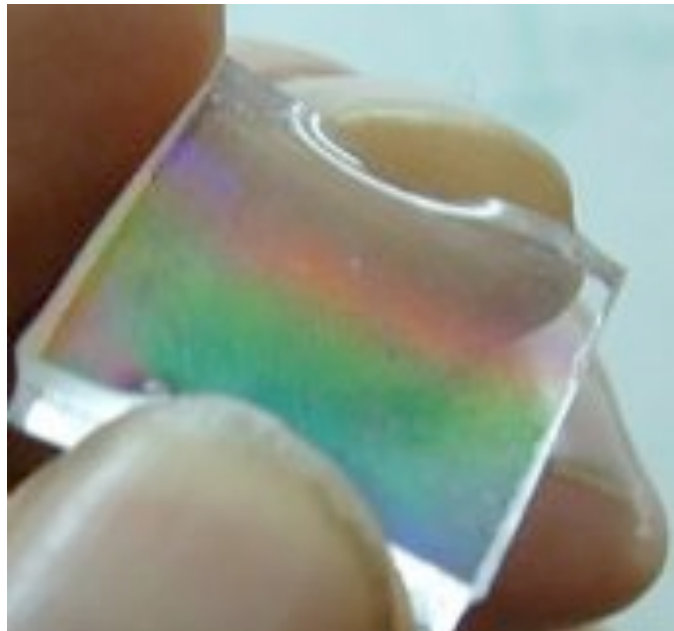


Aperture $\sim 1.08 \mu\text{m}$

Types of Micro-Models: Soft Lithography



“An elastomeric block with patterned relief structures on its surface is the key to soft lithography.” (Xia & Whitesides, 1998)



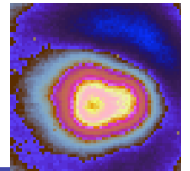
http://www.ws.chemie.tu-muenchen.de/uploads/pics/pdms300_01.jpg

Most Common Elastomer:

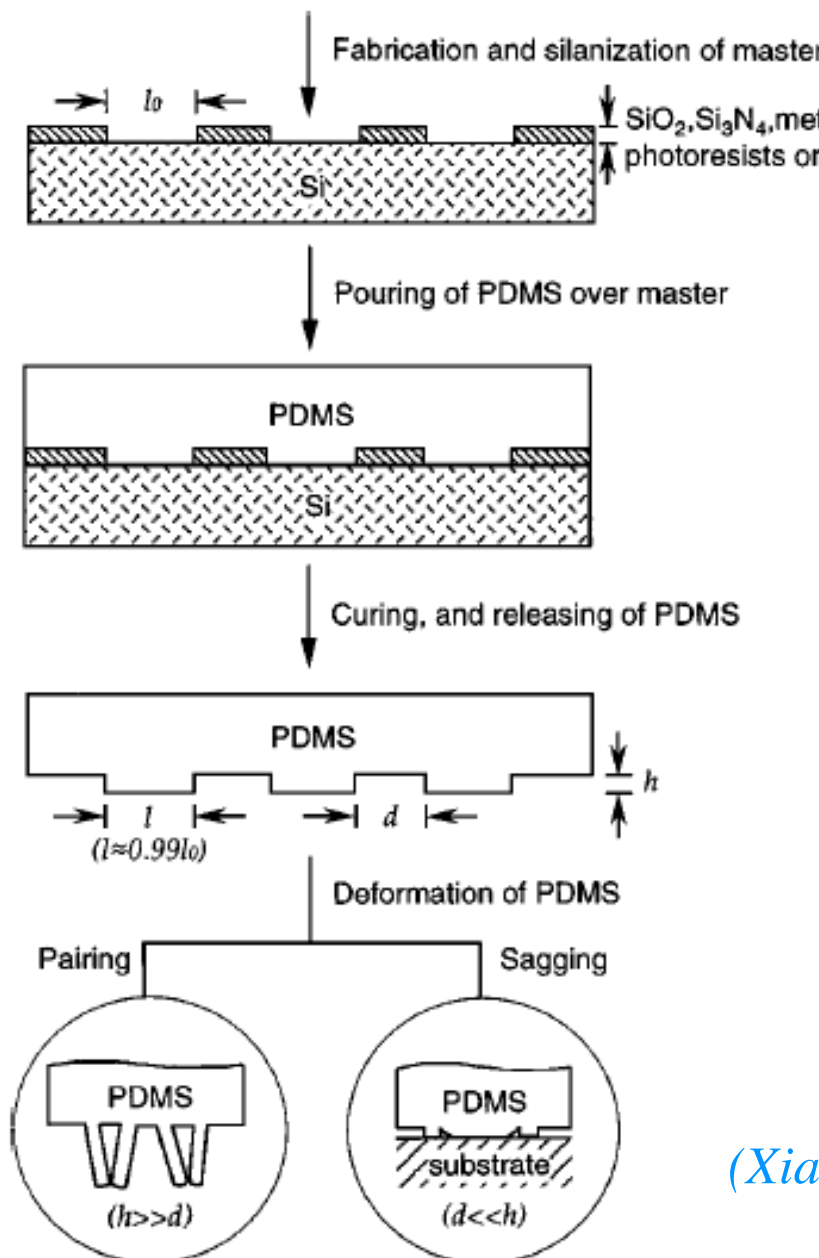
PDMS: Poly(dimethylsiloxane)

Other Elastomers:

polyurethanes, polyimides,
phenol formaldehyde polymer

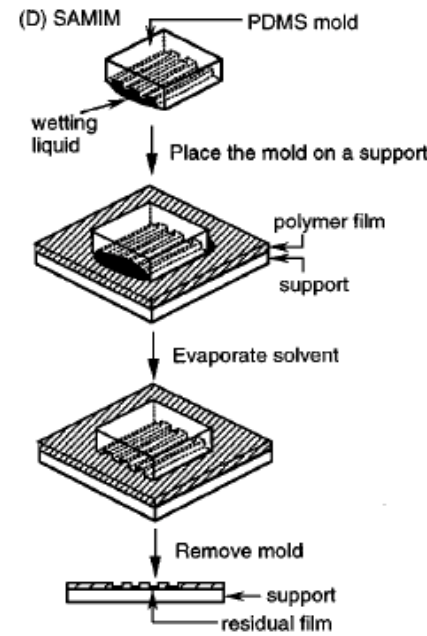
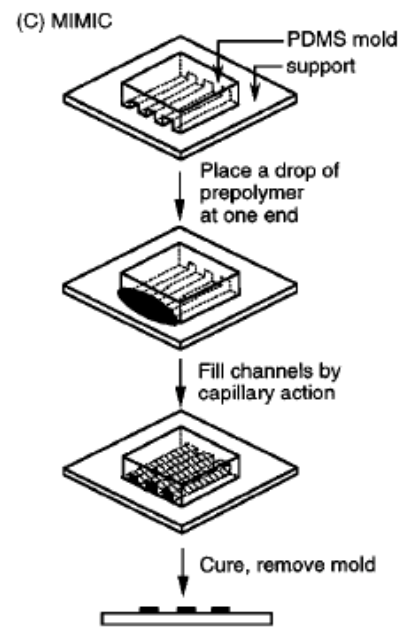
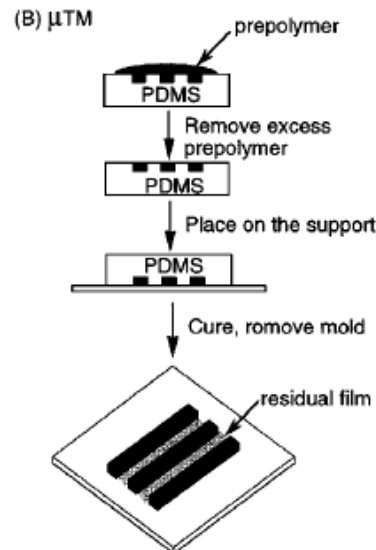
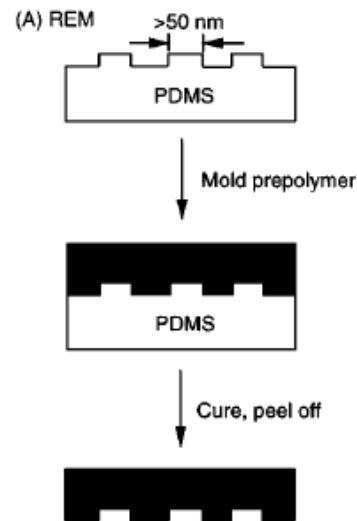
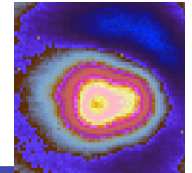


Types of Micro-Models: Soft Lithography

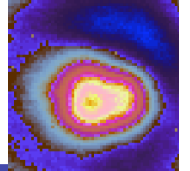


(Xia & Whitesides, 1998)

Types of Micro-Models: Soft Lithography

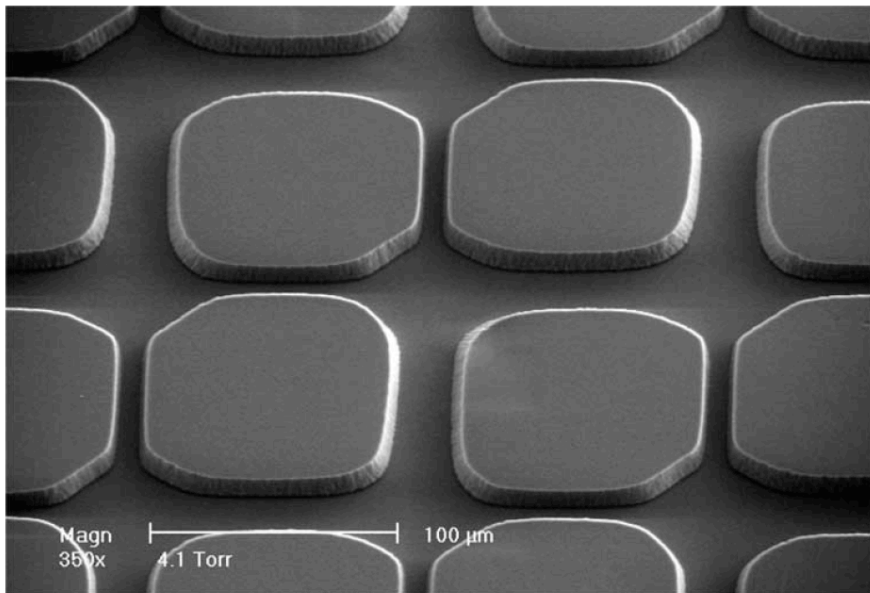


(Xia & Whitesides, 1998)



Types of Micro-Models: Soft Lithography

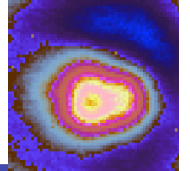
PDMS: Example from Hydrology Community



Auset & Keller, 2004

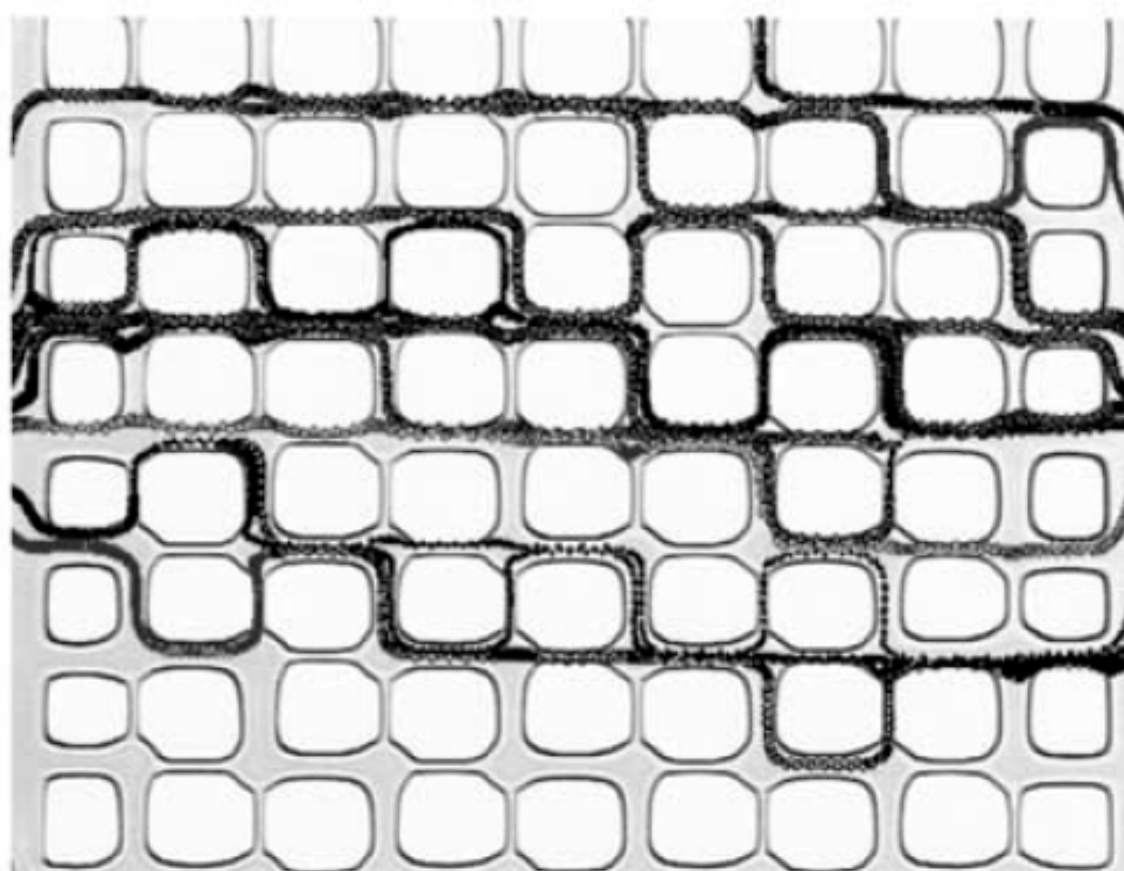
Table 1. Physical and Hydraulic Properties of Micromodels

	Micromodel		
	A	B	C
Length, mm	1	1	1
Width, mm	0.8	0.8	0.8
Porosity	0.228	0.358	0.278
Thickness, mm	1.2×10^{-2}	1.2×10^{-2}	1.2×10^{-2}
Pore volume, mm ³	2.7×10^{-3}	4.3×10^{-3}	3.3×10^{-3}
Permeability, mm ²	1.2×10^{-6}	6.2×10^{-6}	2.6×10^{-6}



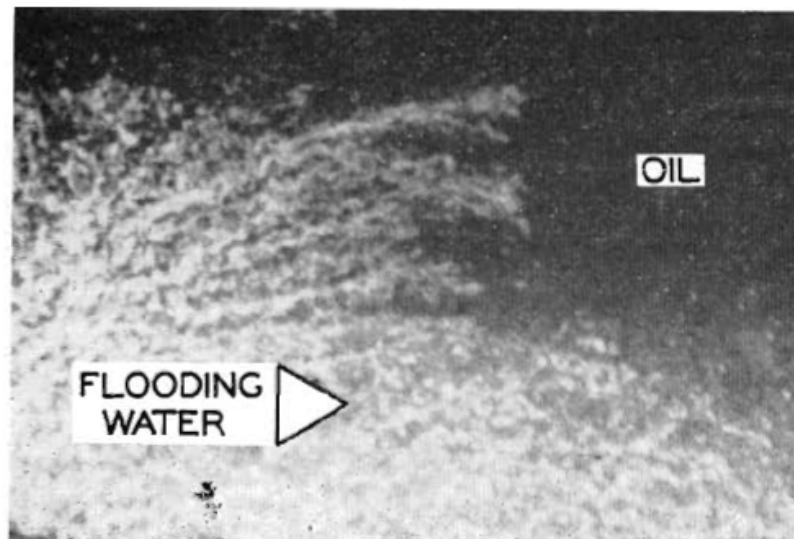
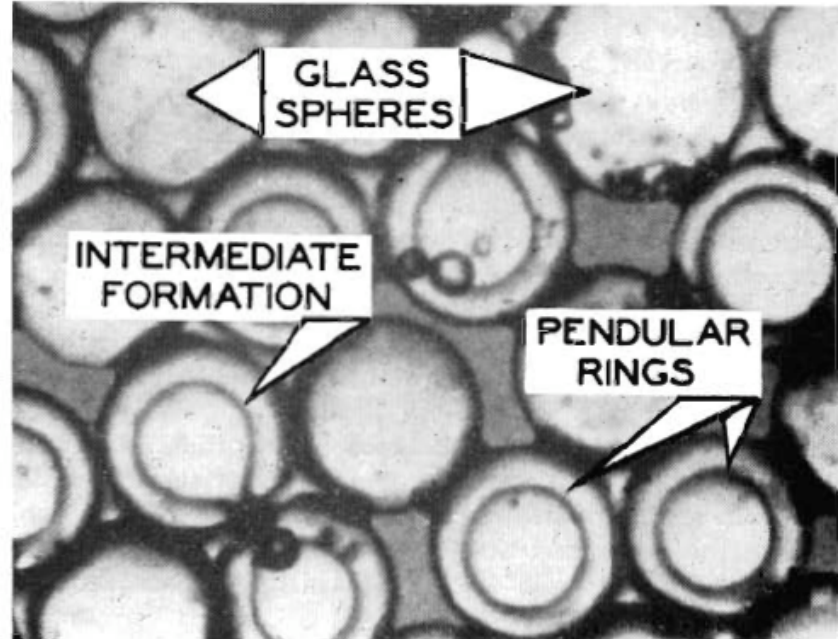
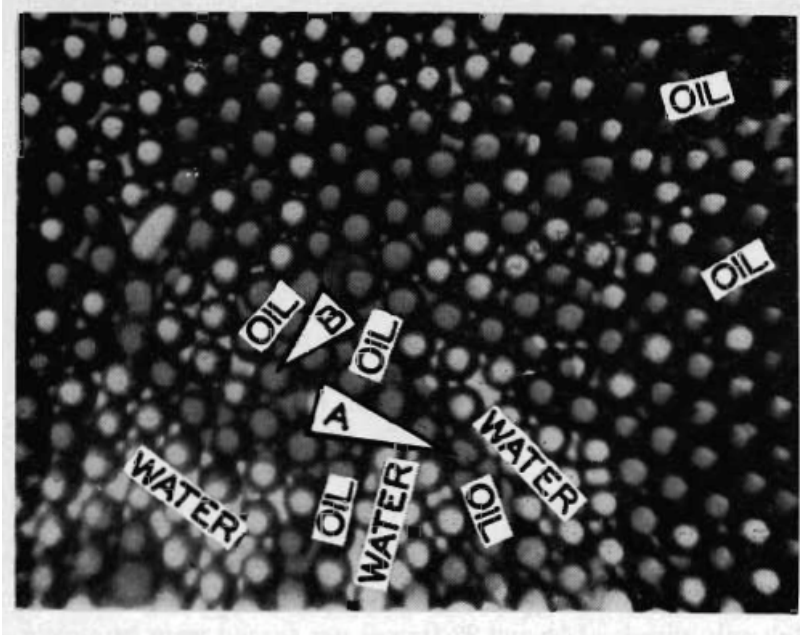
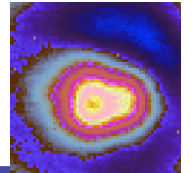
Types of Micro-Models: Soft Lithography

PDMS: Example from Hydrology Community



Auset & Keller, 2004

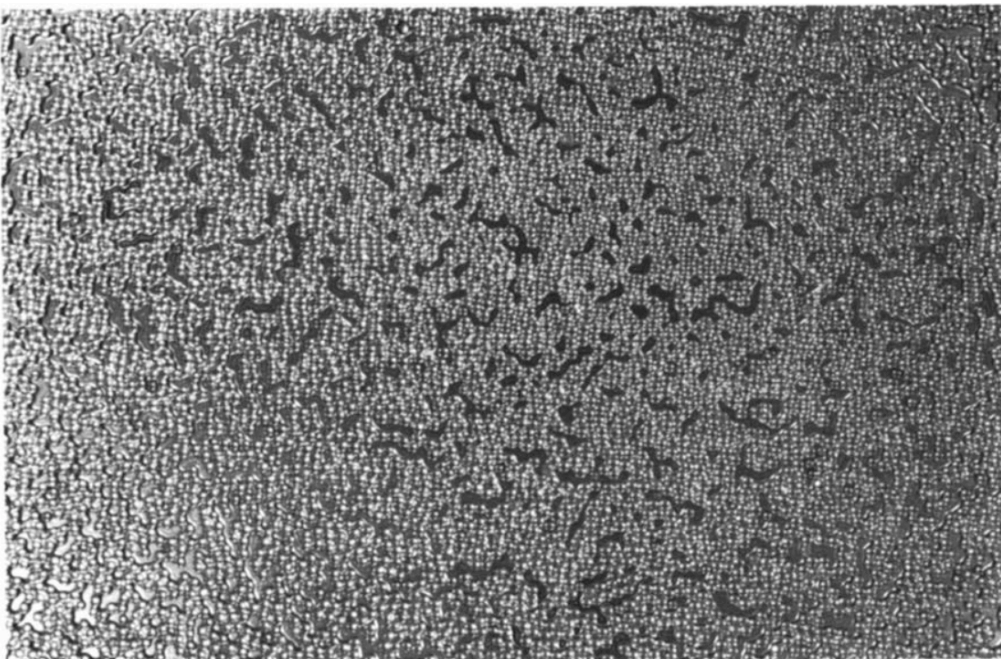
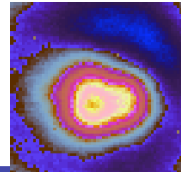
Types of Micro-Models: Glass Beads



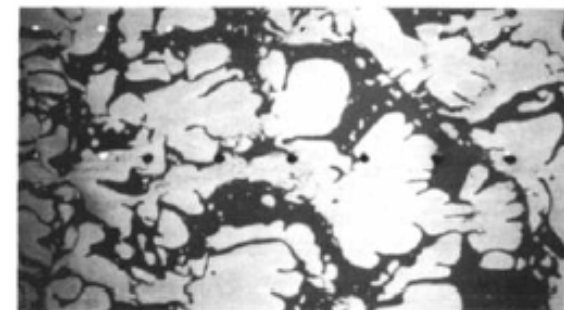
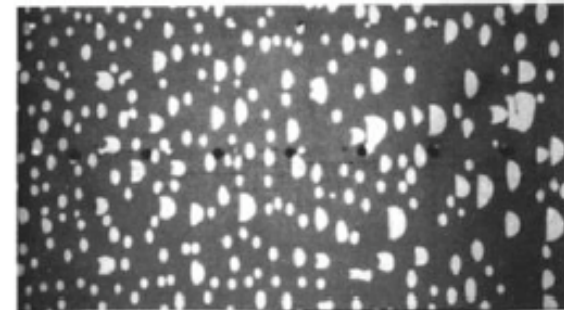
(*Chatenever & Calhoun, 1952*)

One layer of 178 microns in diameter spherical glass beads

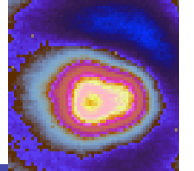
Types of Micro-Models: Glass Beads



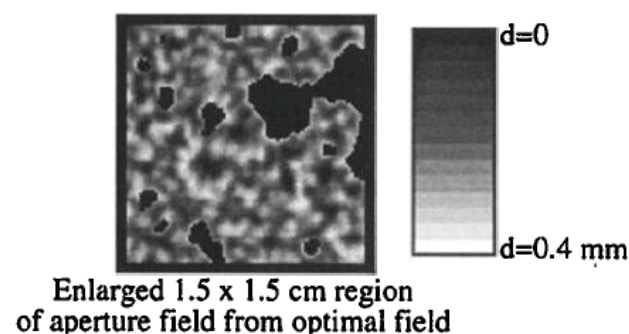
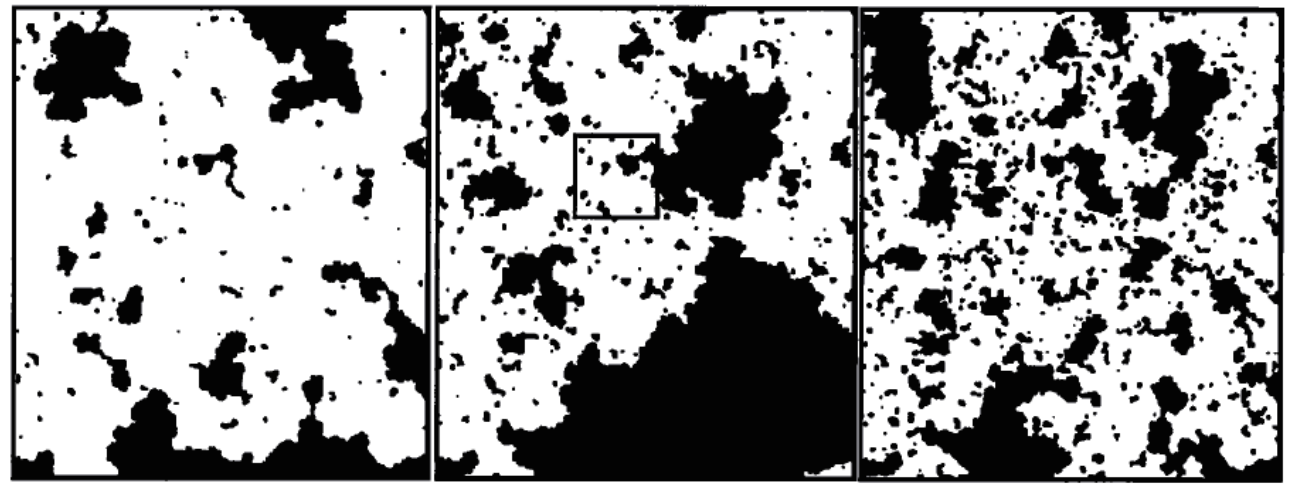
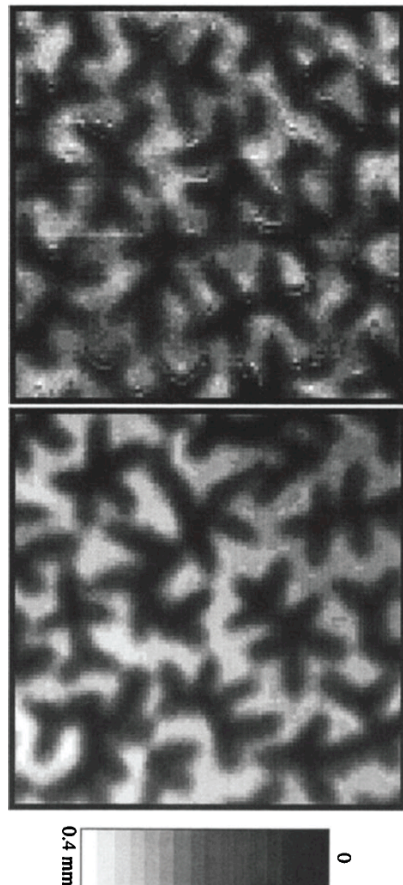
1 mm glass spheres



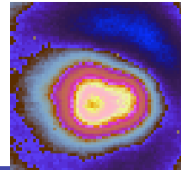
Types of Micro-Models: Simulacrum



Detwiler et al., 1999



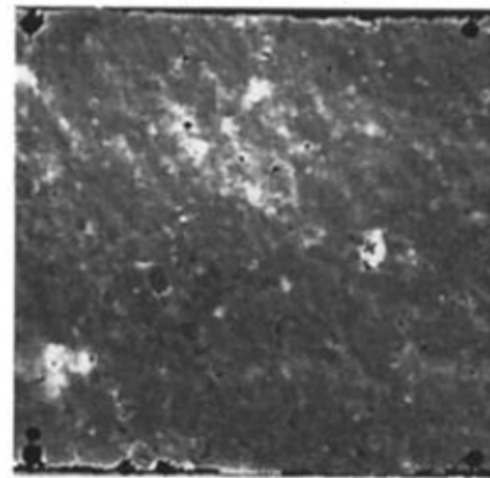
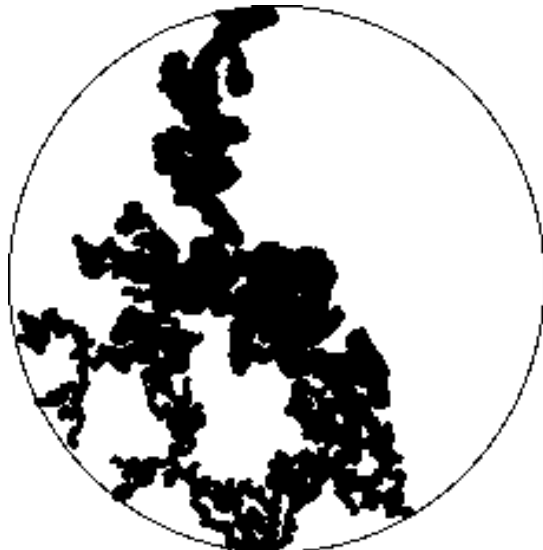
Types of Micro-Models: Replicas



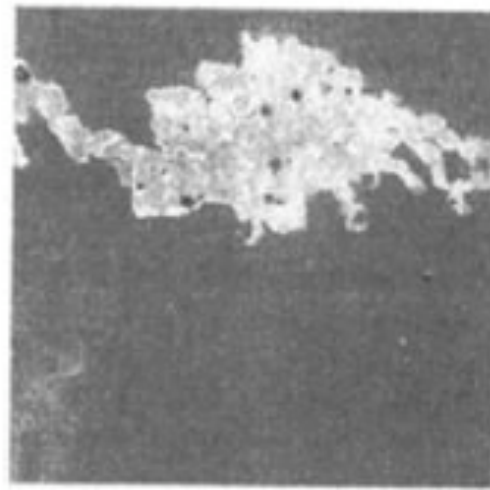
Brown et al., 1998

Fracture Casts

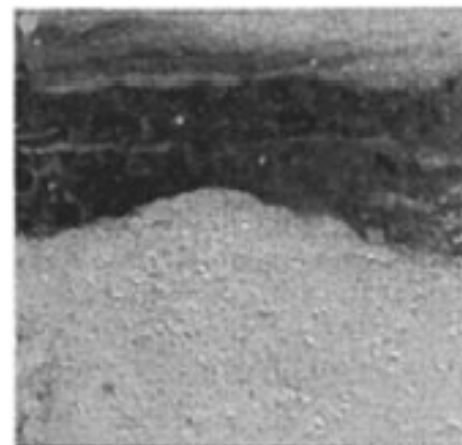
Pyrak-Nolte et al., 1992



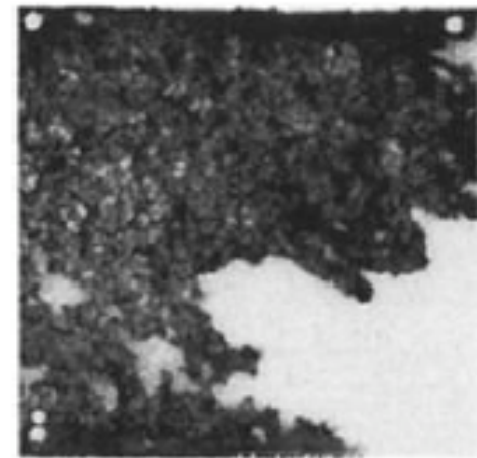
Dry Fracture



Air Invasion



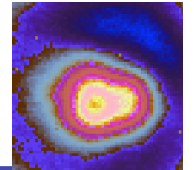
Dye



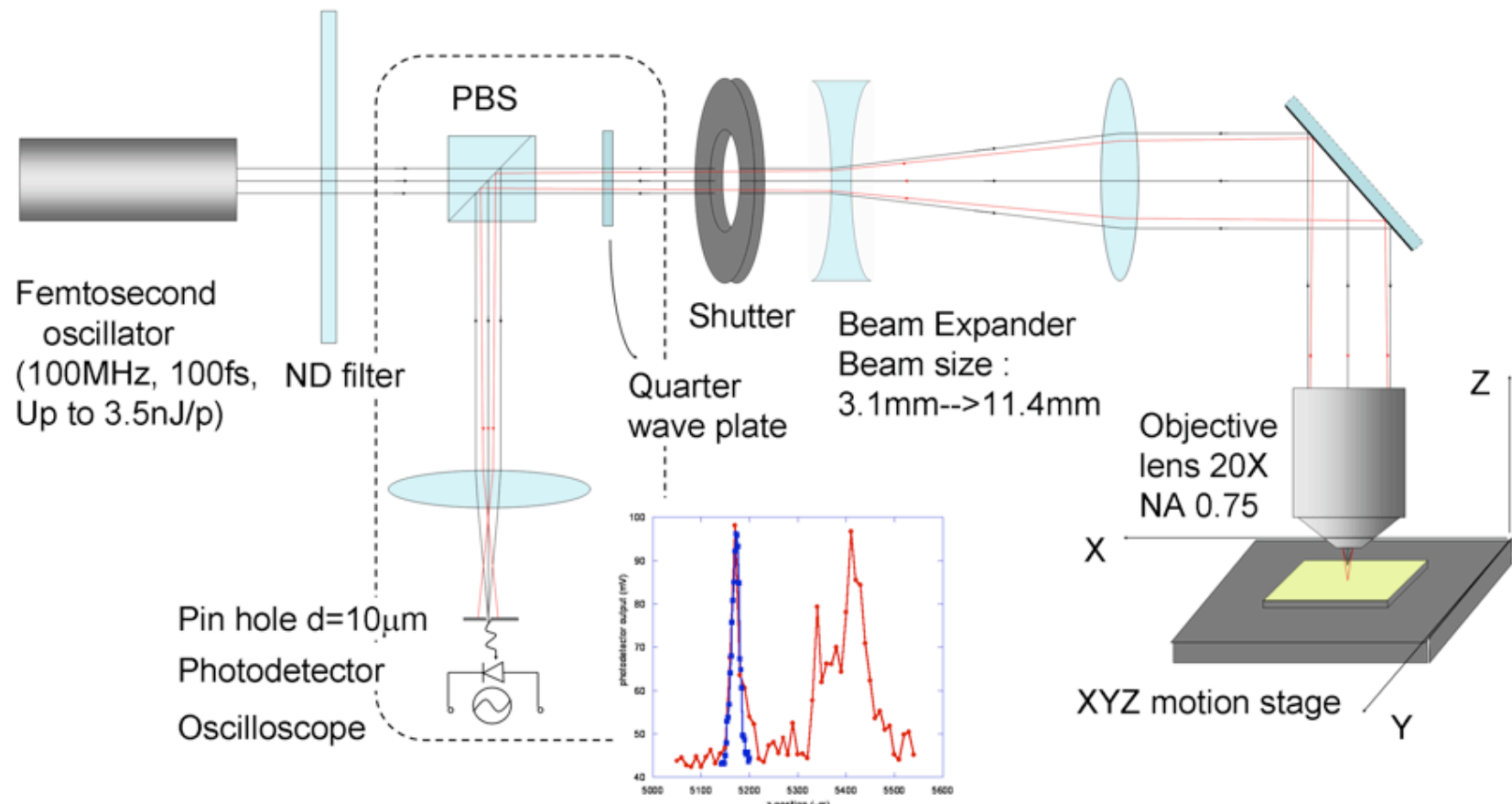
Water Invasion

Pyrak-Nolte

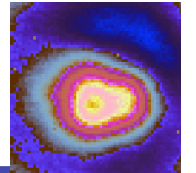
Micro-Models: Toward Three-Dimensions



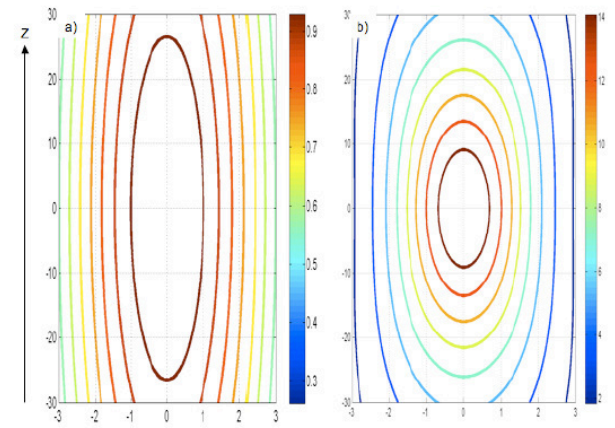
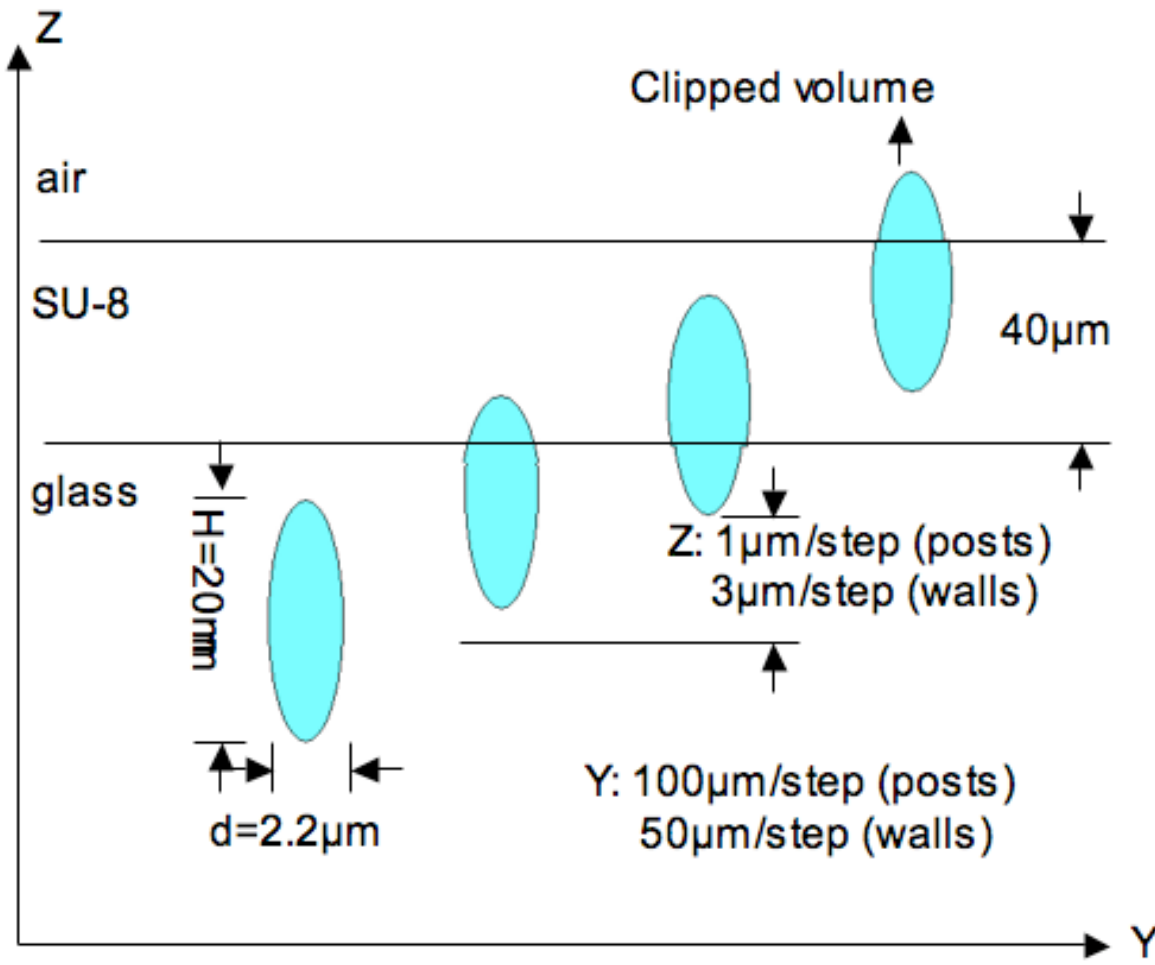
*Two Photon Adsorption Lithography



Micro-Models: Toward Three-Dimensions



*Two Photon Adsorption Lithography

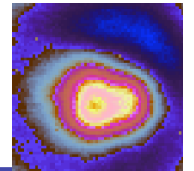


$$I^2 \beta \tau v t \geq F_{th}$$

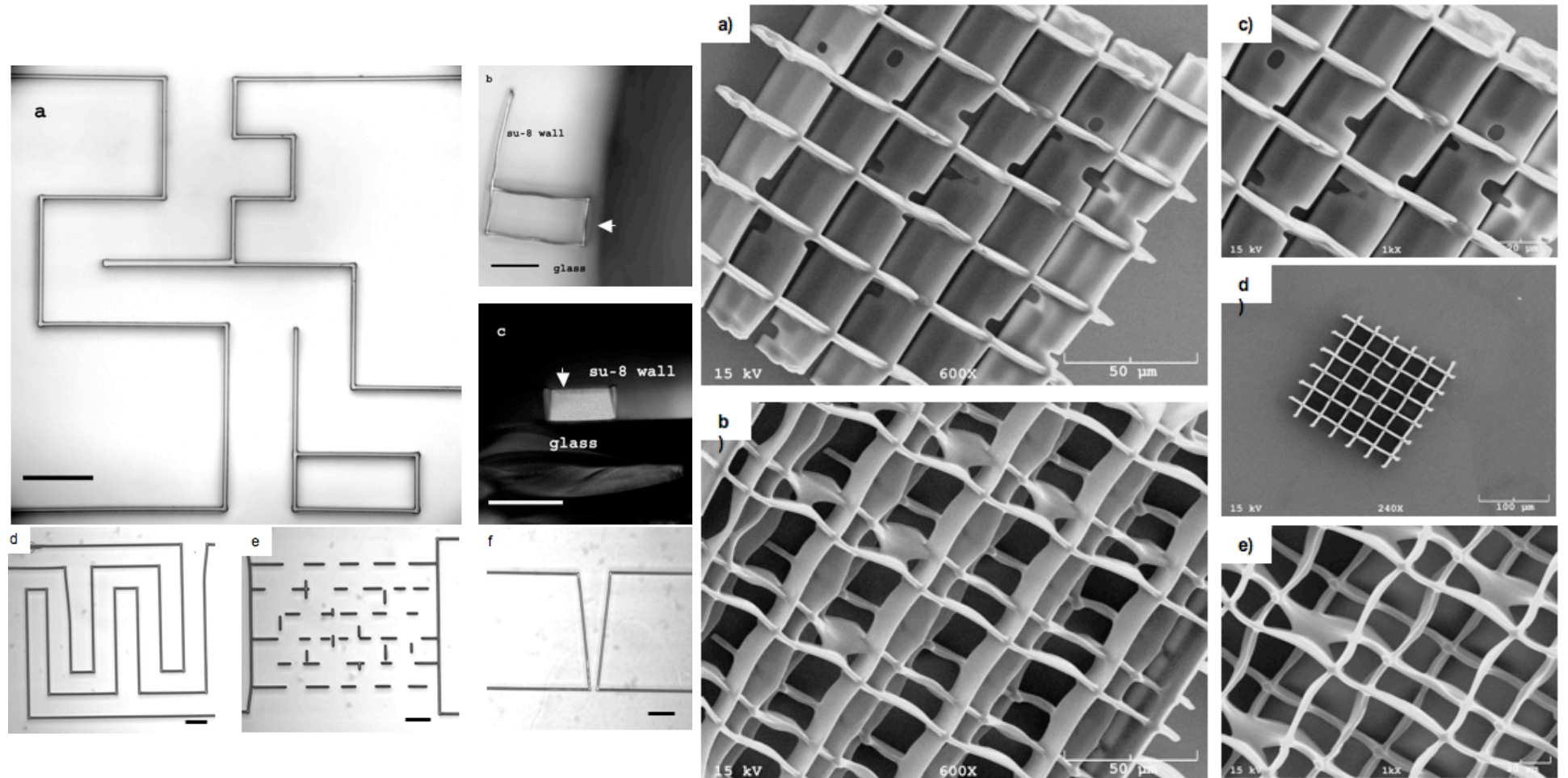
$$d = w_o \sqrt{\ln\left(\frac{I_o^2 t \beta \tau v}{F_{th}}\right)}$$

$$H = \frac{2z_r}{n} \sqrt{\exp\left(\frac{1}{2} \frac{d^2}{w_o^2}\right) - 1}$$

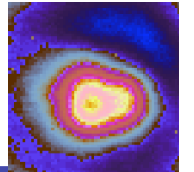
Micro-Models: Toward Three-Dimensions



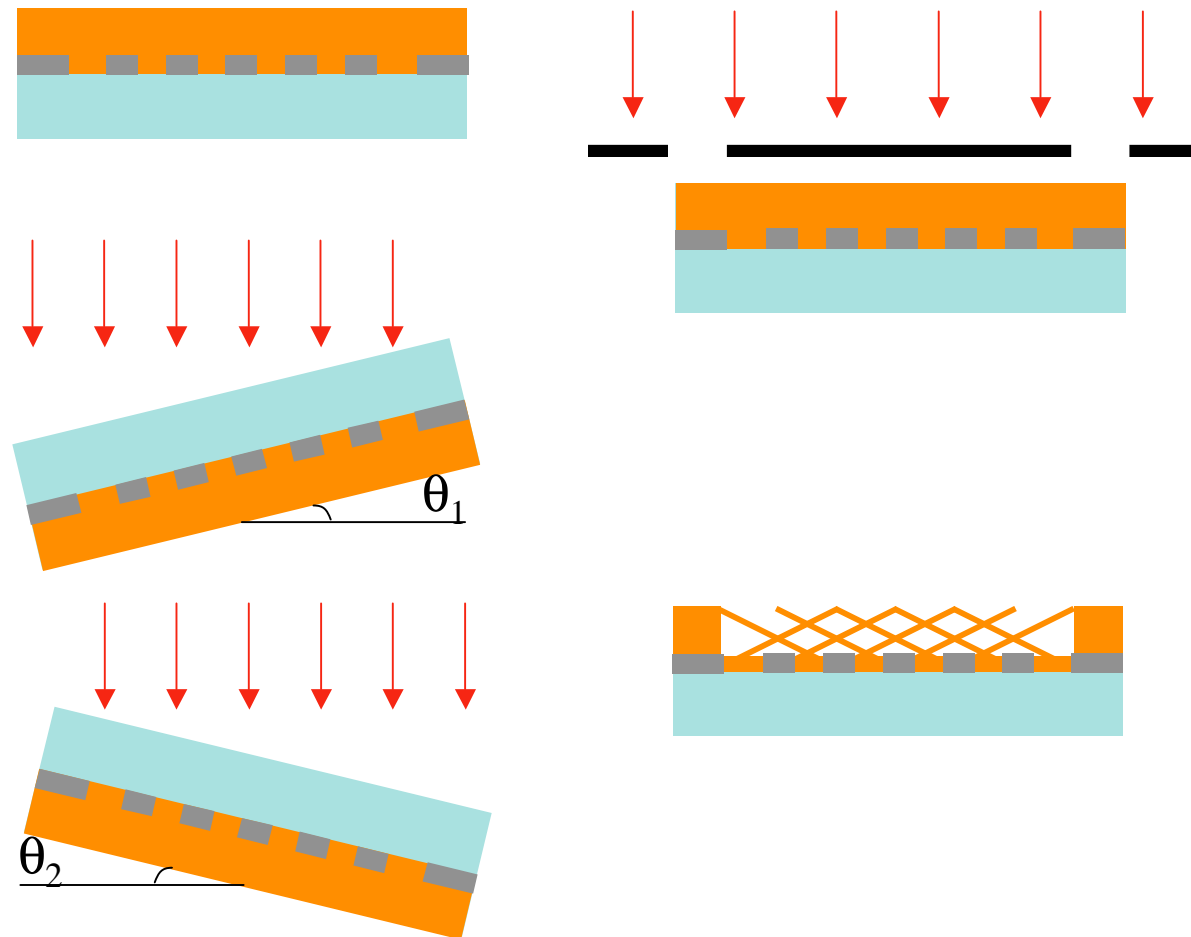
*Two Photon Adsorption Lithography

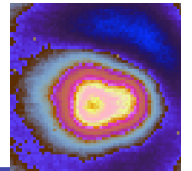


Micro-Models: Three-Dimensions



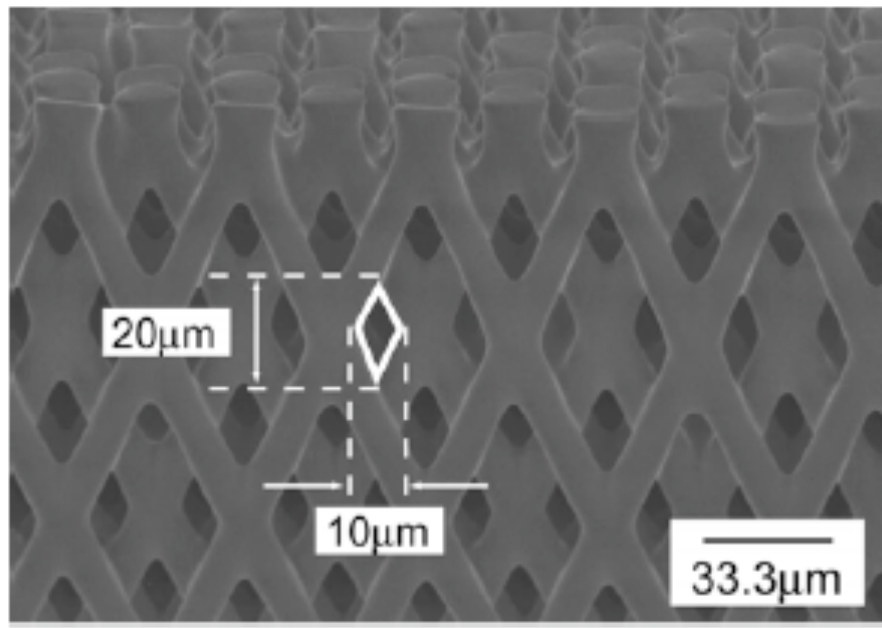
*High Angle Exposure



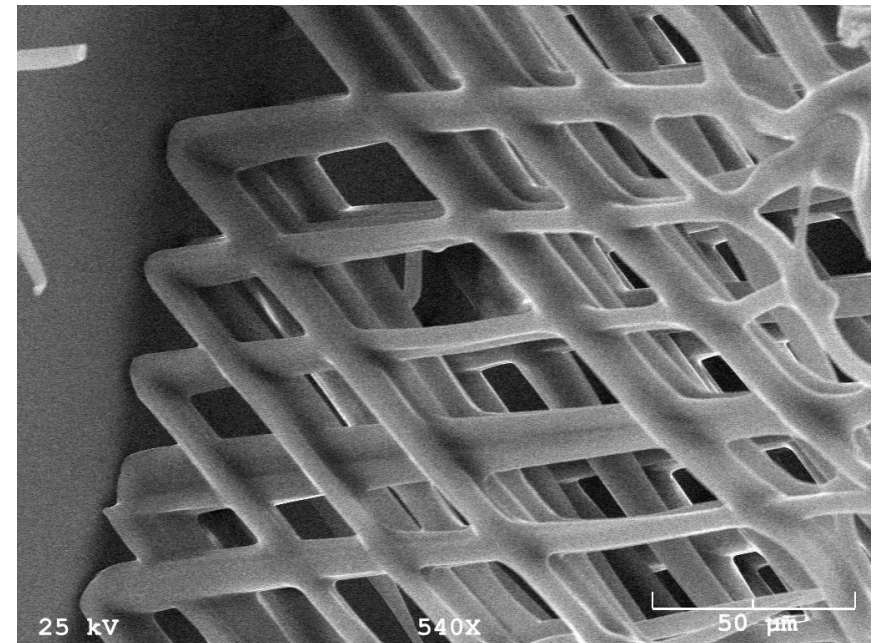


Micro-Models: Three-Dimensions

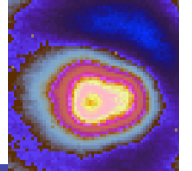
*High Angle Exposure



(Sato et al., 2003)



(Liu 2009-2010 in progress)

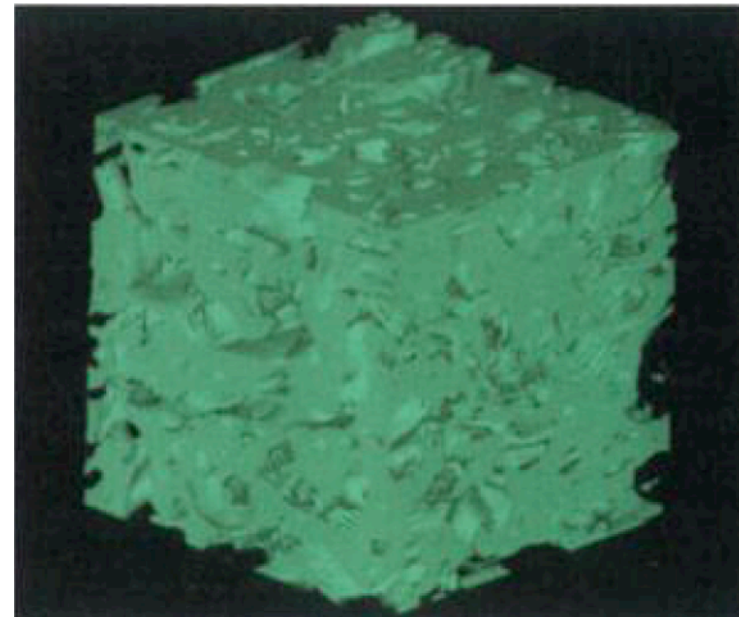
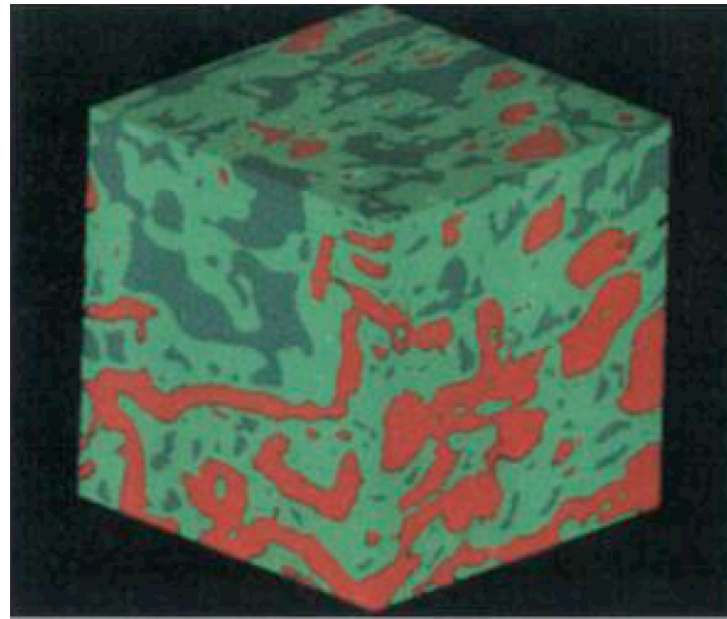


Micro-Models: Three-Dimensional

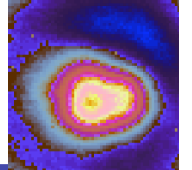
*Optical quality glass sand

*Index matched fluids

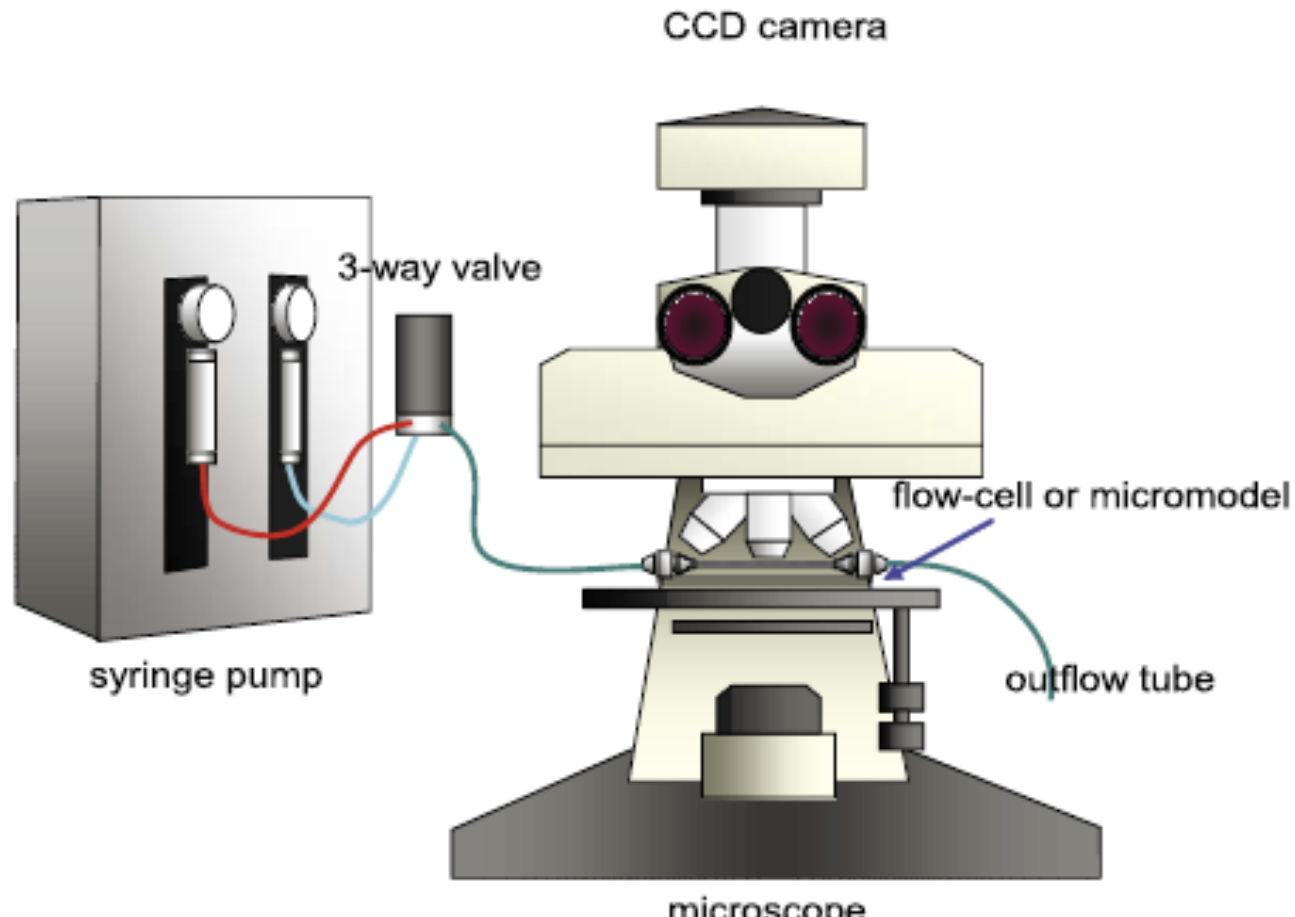
*Fluorophores



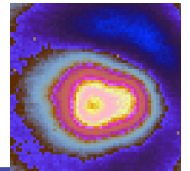
Montemagno & Gray, 1995



Imaging Systems: Optical Microscope



(from Ochiai et al., 2006)



Imaging Systems: Visualization Chambers

*Sand packs, fracture replicas

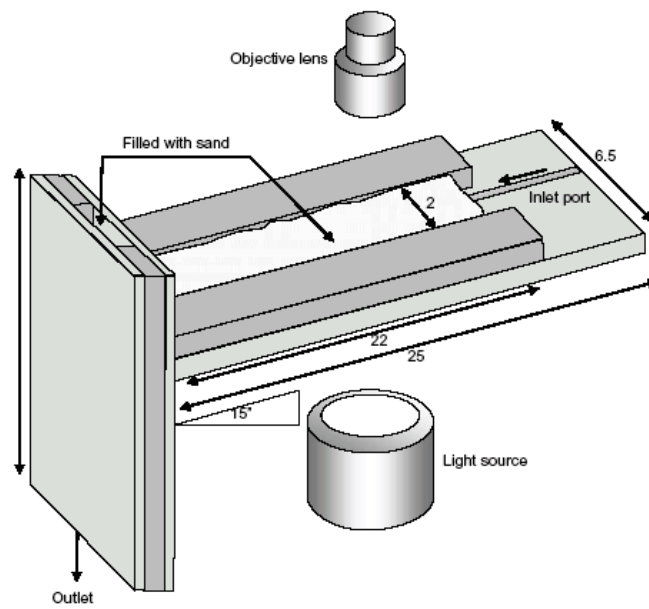


Figure 5. Schematic of tilted, open-faced visualization chamber utilized by Crist *et al.* [2004, 2005] and Zevi *et al.* [2005], showing chamber dimensions and positioning of video magnification lens and light source. Adapted with permission from Zevi *et al.* [2005]. Copyright 2005 American Chemical Society.

(from Ochiai *et al.*, 2006)

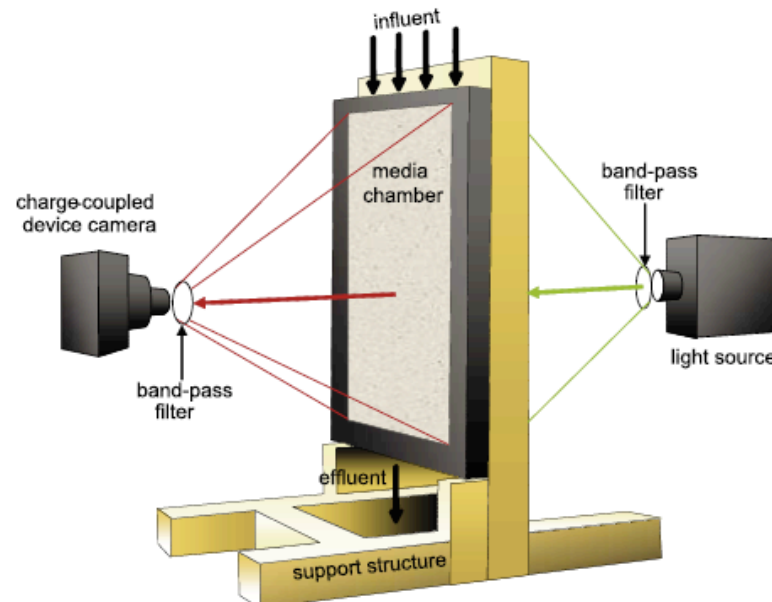
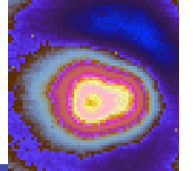
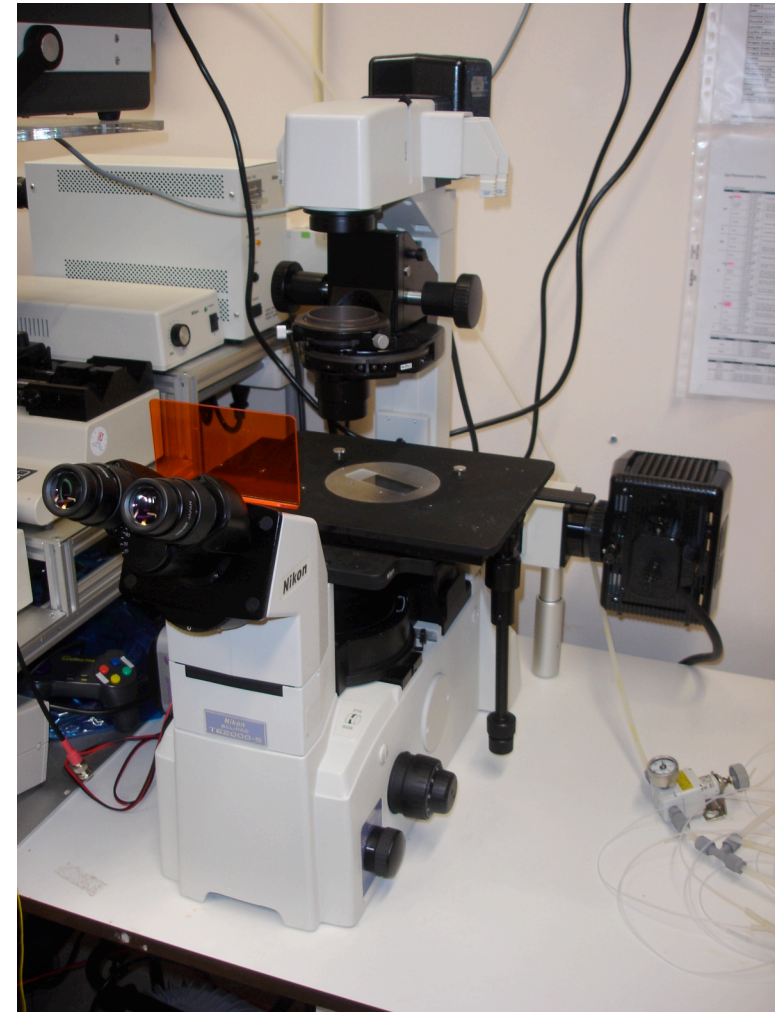
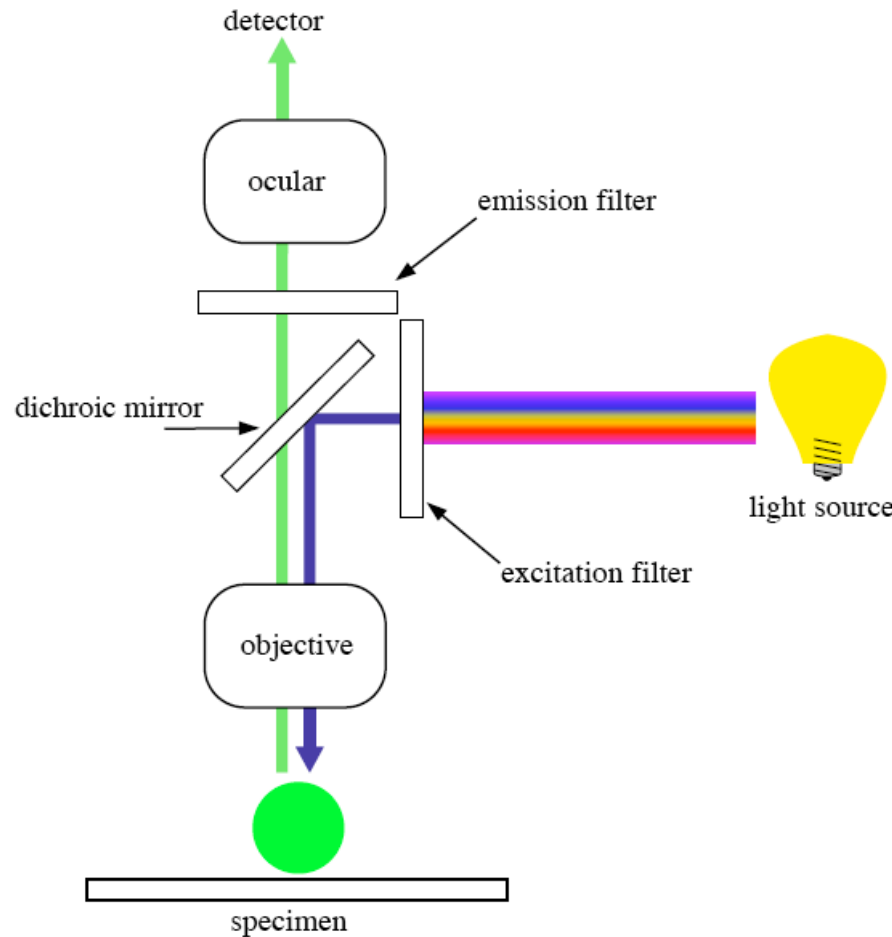


Figure 9. Schematic of mesoscale light transmission visualization under development by Kraft and Selker [2005], showing arrangement of optical components and media chamber. Note: not drawn to scale.

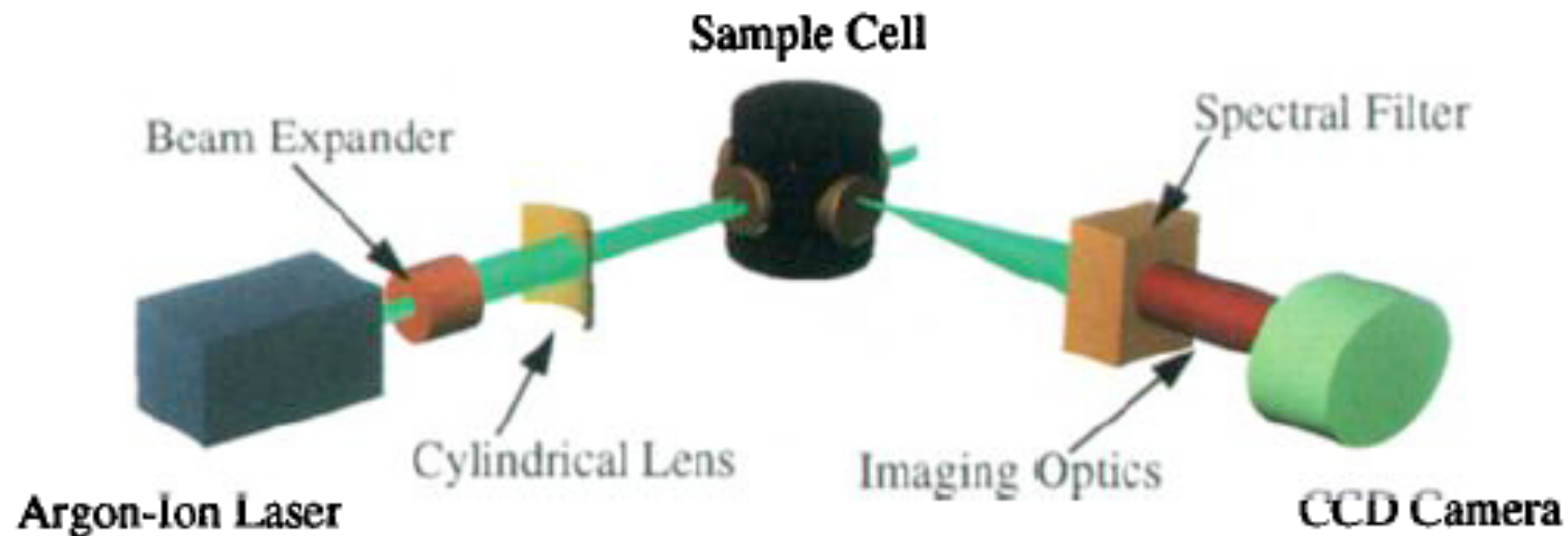
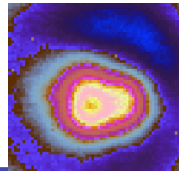


Imaging Systems: Epifluorescence Microscope

Example: Nikon TE2000

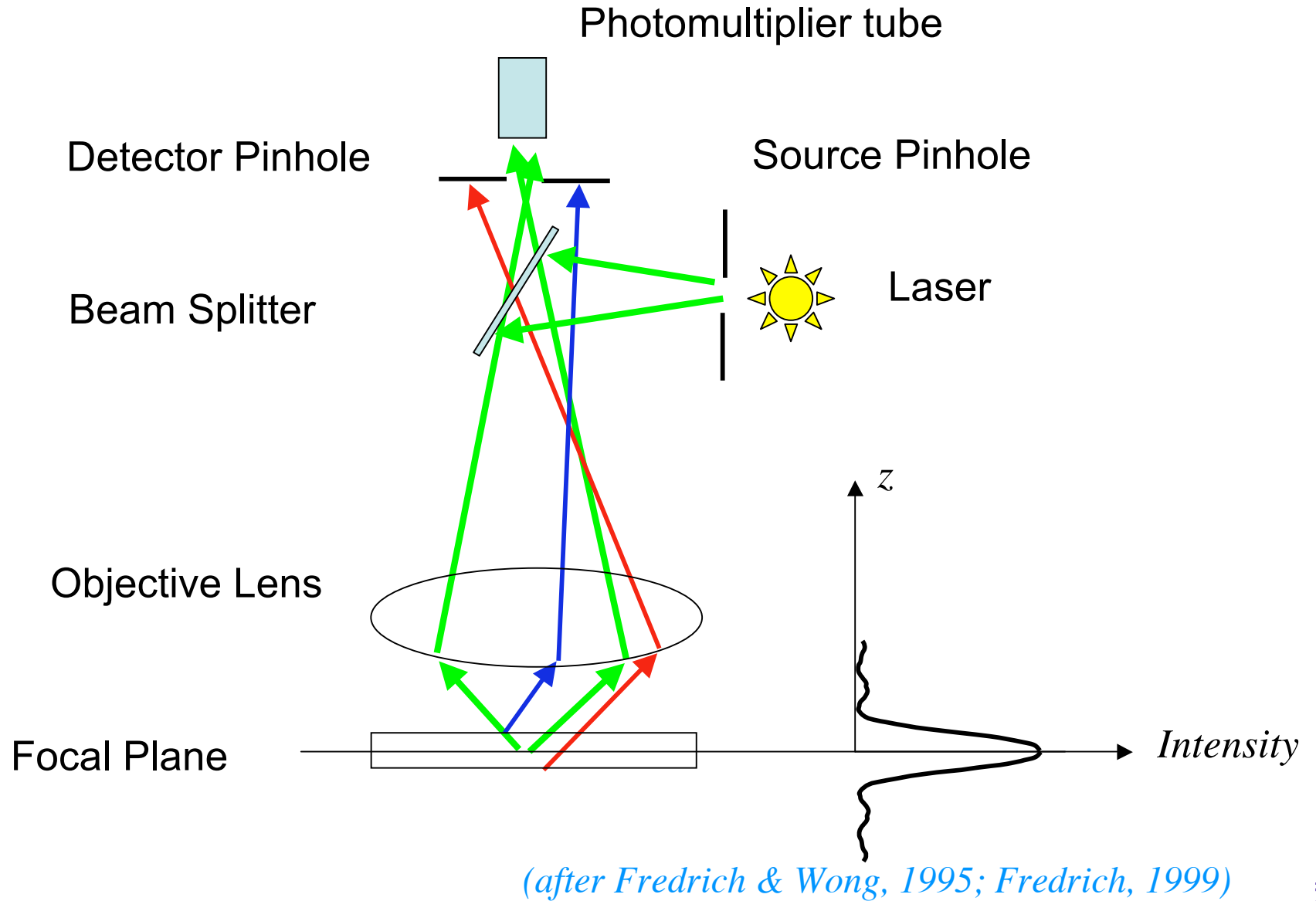
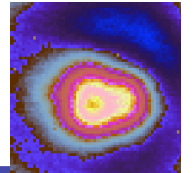


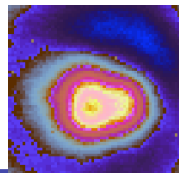
Imaging Systems: PVI



Montemagno & Gray, 1995

Imaging Systems: Laser Confocal Microscopy





Laser Confocal Microscopy

Table 1. Lateral resolution R (Eq. 1) and optical section thickness at $\lambda=514 \text{ nm}$ for various settings of the confocal aperture

Objective	M	NA	R (μm)	Section thickness (μm)			
				Open	1/3	2/3	Closed
$\times 10$		0.45	0.71	38	25	13	7.0
$\times 20$		0.75	0.42	14	10	6.7	5.0
$\times 40$		1.0	0.31	6.1	4.2	2.6	1.4
$\times 60$		1.4	0.22	3.7	2.0	1.0	0.7

(Fredrich & Wong, 1995; Fredrich, 1999)

Imaging Systems: Laser Confocal Microscopy

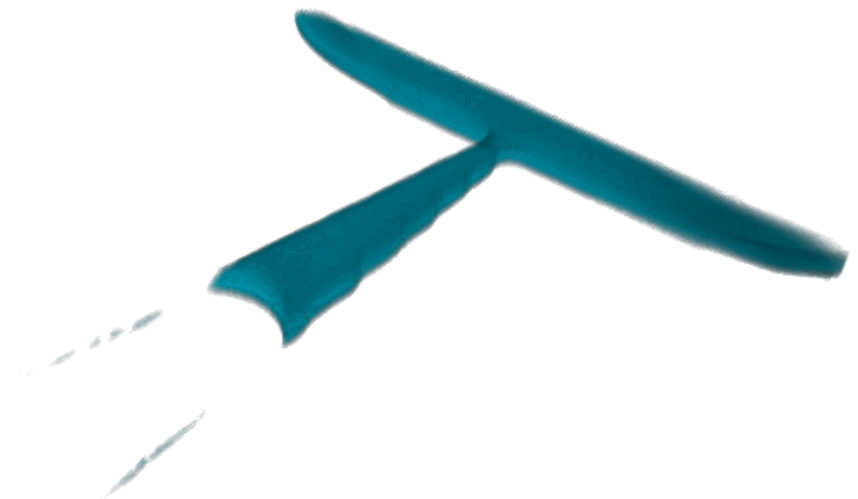
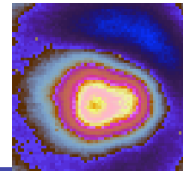
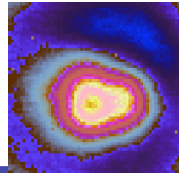


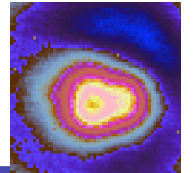
Image Analysis



From Image Analysis:

- ❖ Saturation
- ❖ Interfacial Length
- ❖ Curvature
- ❖ Normals to Interfaces

Image Analysis: Phase Identification



Non-Uniform Lighting

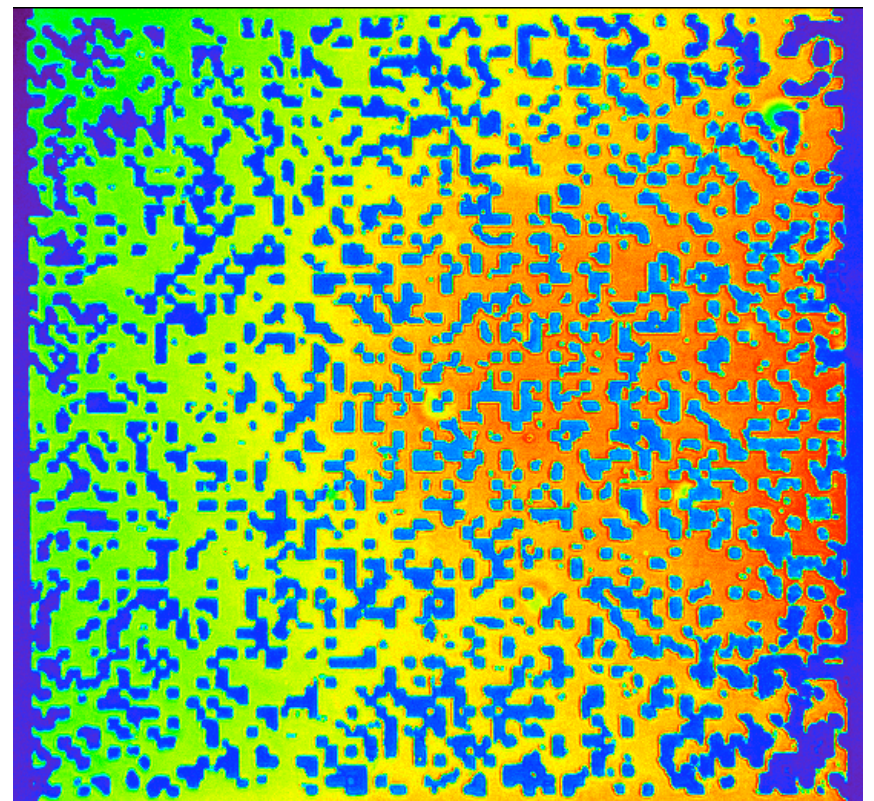
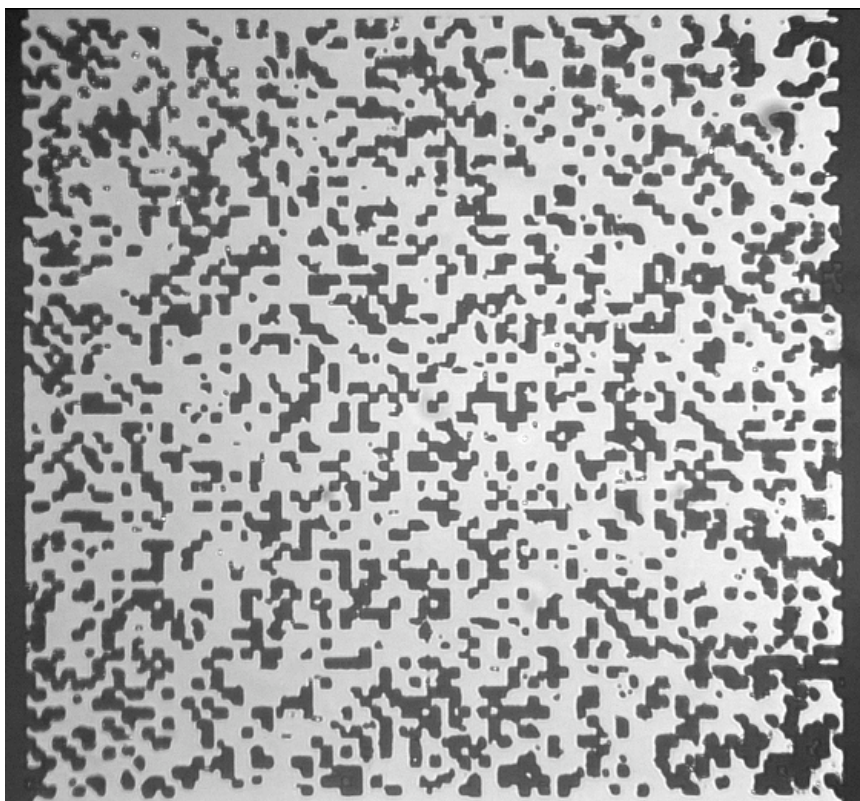
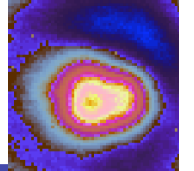


Image Analysis: Phase Identification



$$function = a * (x - x_{ic})^2$$

$$Newimage = image + function$$

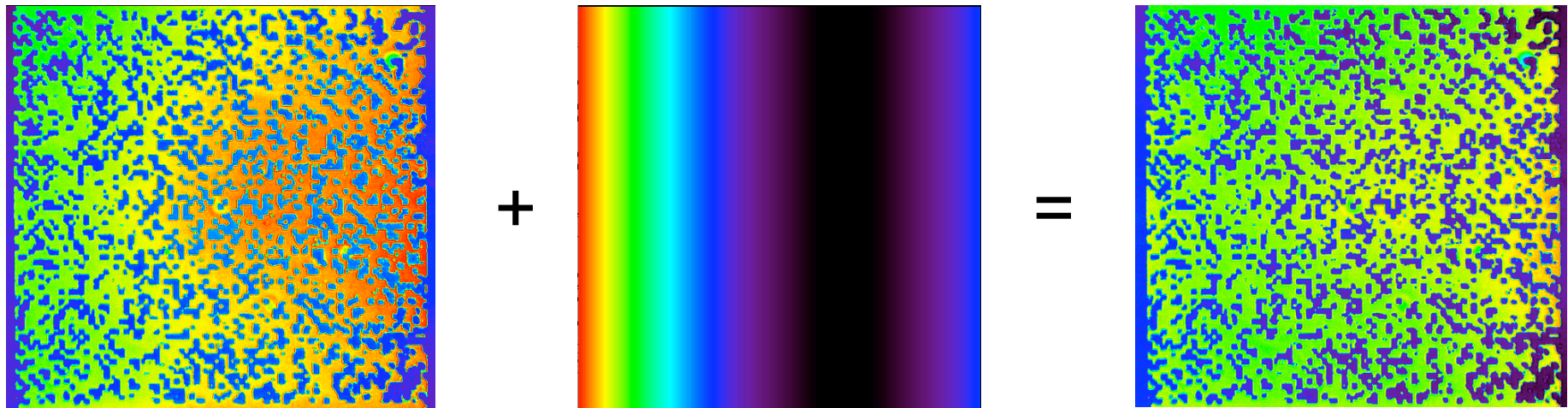
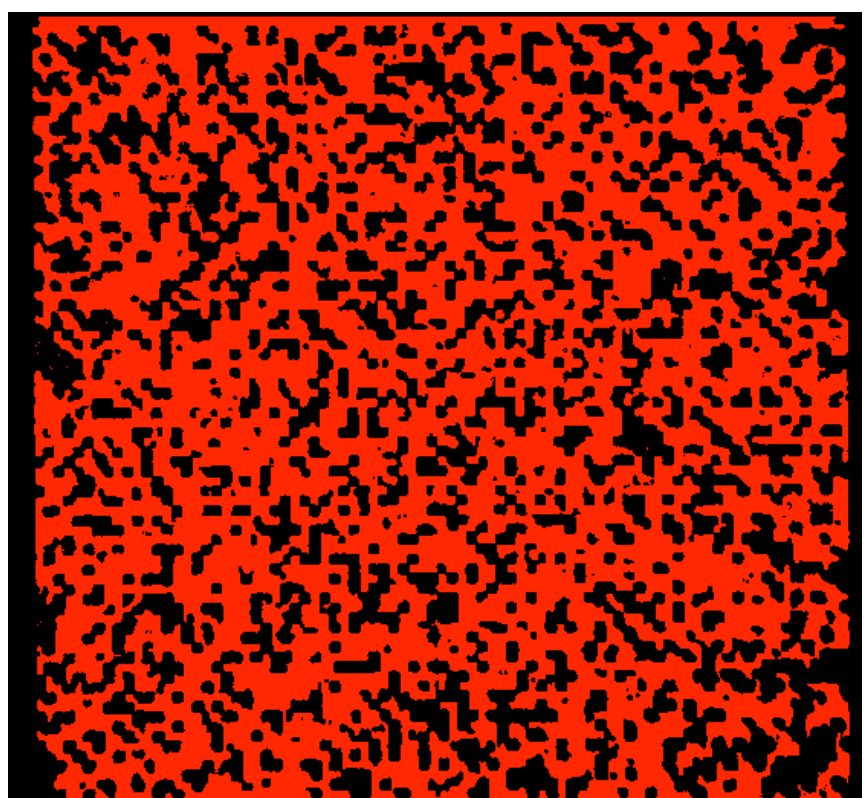
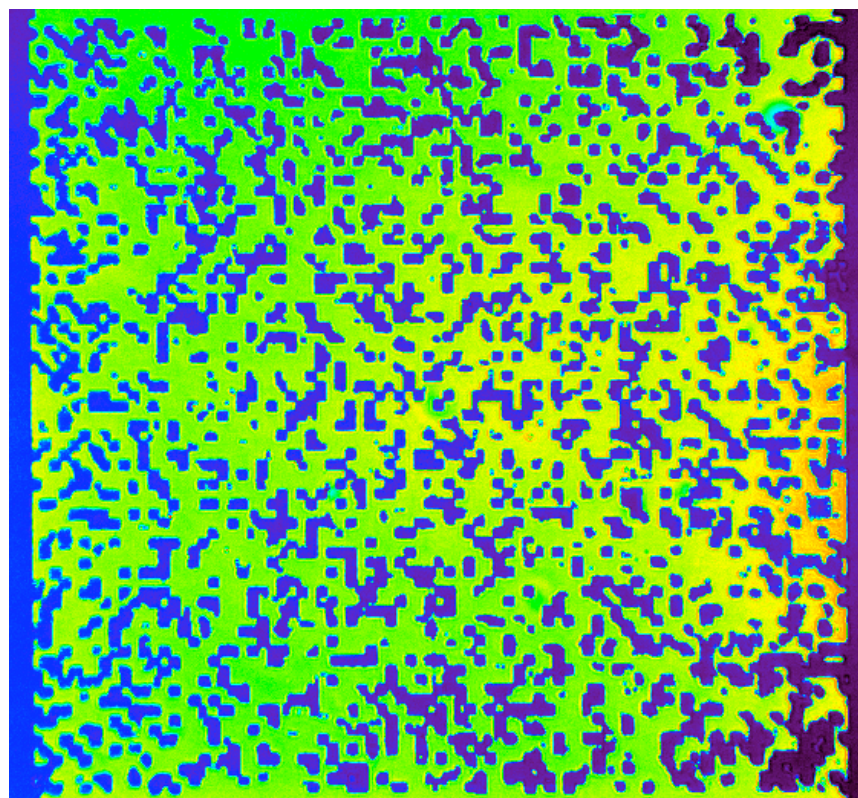
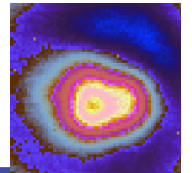


Image Analysis: Connected Path



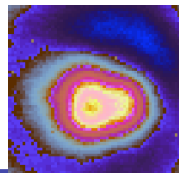
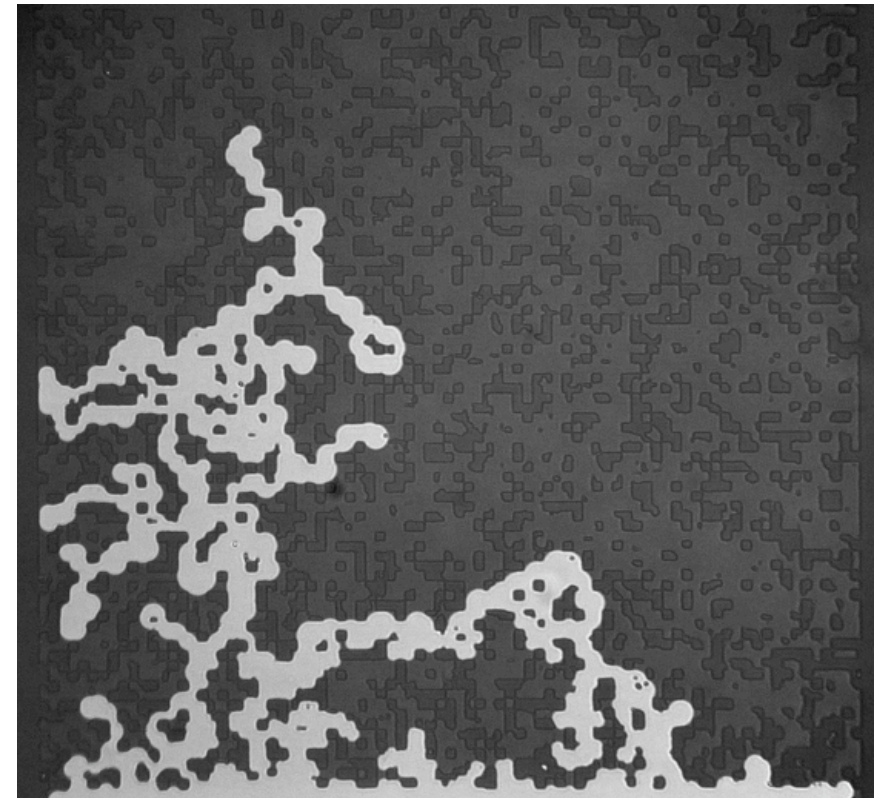
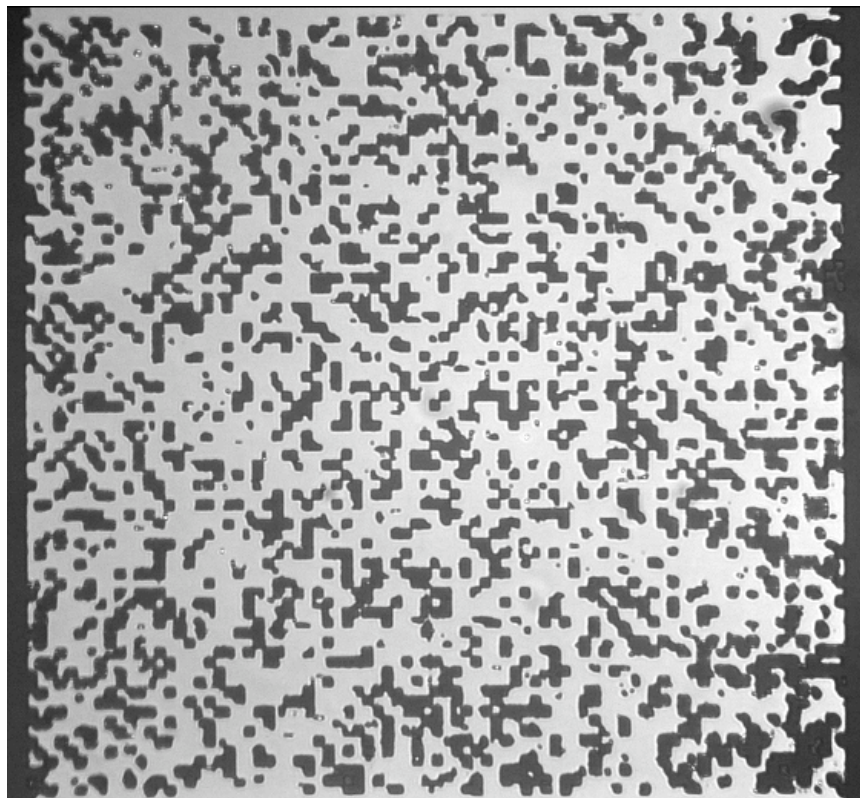


Image Registration: Cross-Correlation

$$S_2(x, y) = \frac{1}{A} \int_A f_{mask}(u, v) f_{image}(u - x, v - y) du dv$$



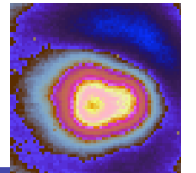


Image Registration: Cross-Correlation

$$S_2(x, y) = \frac{1}{A} \int_A f_{mask}(u, v) f_{image}(u - x, v - y) du dv$$

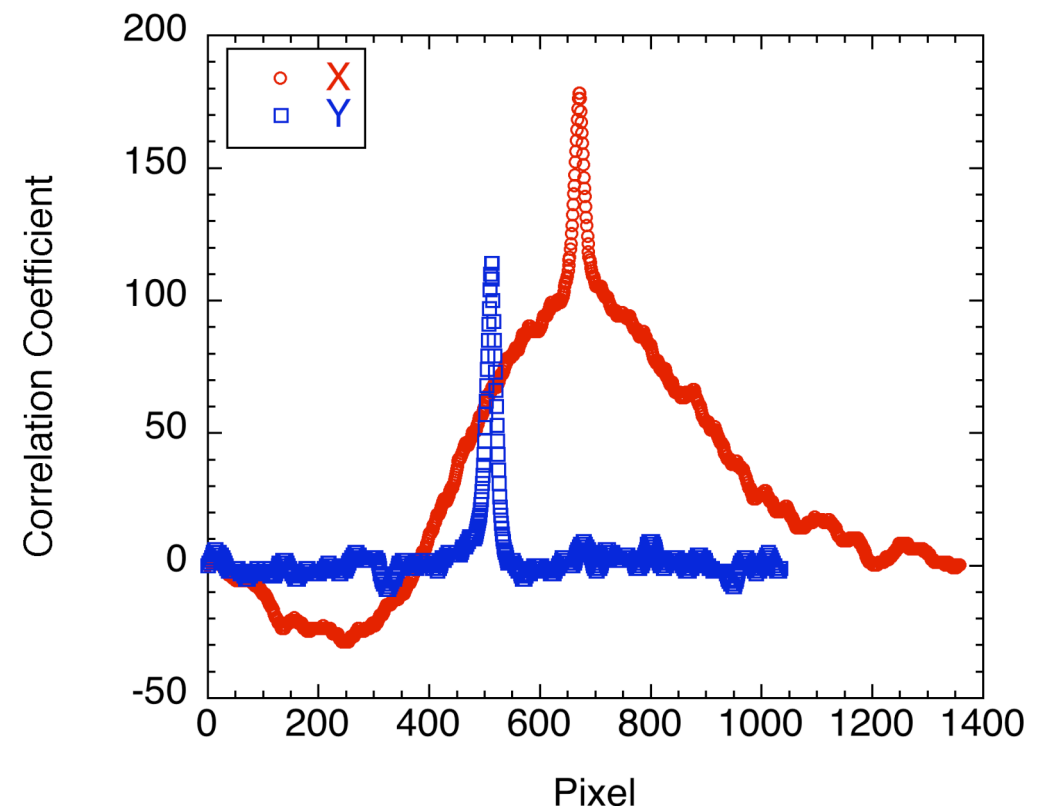
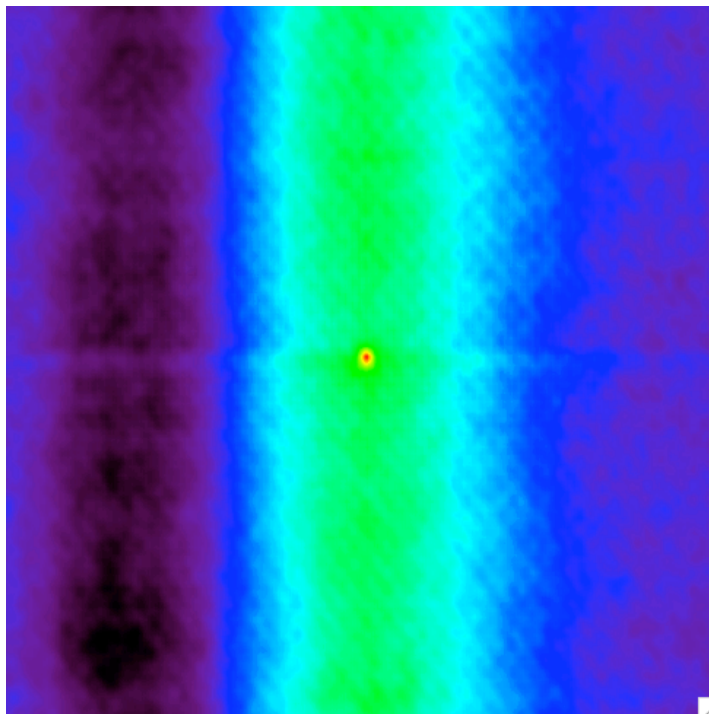
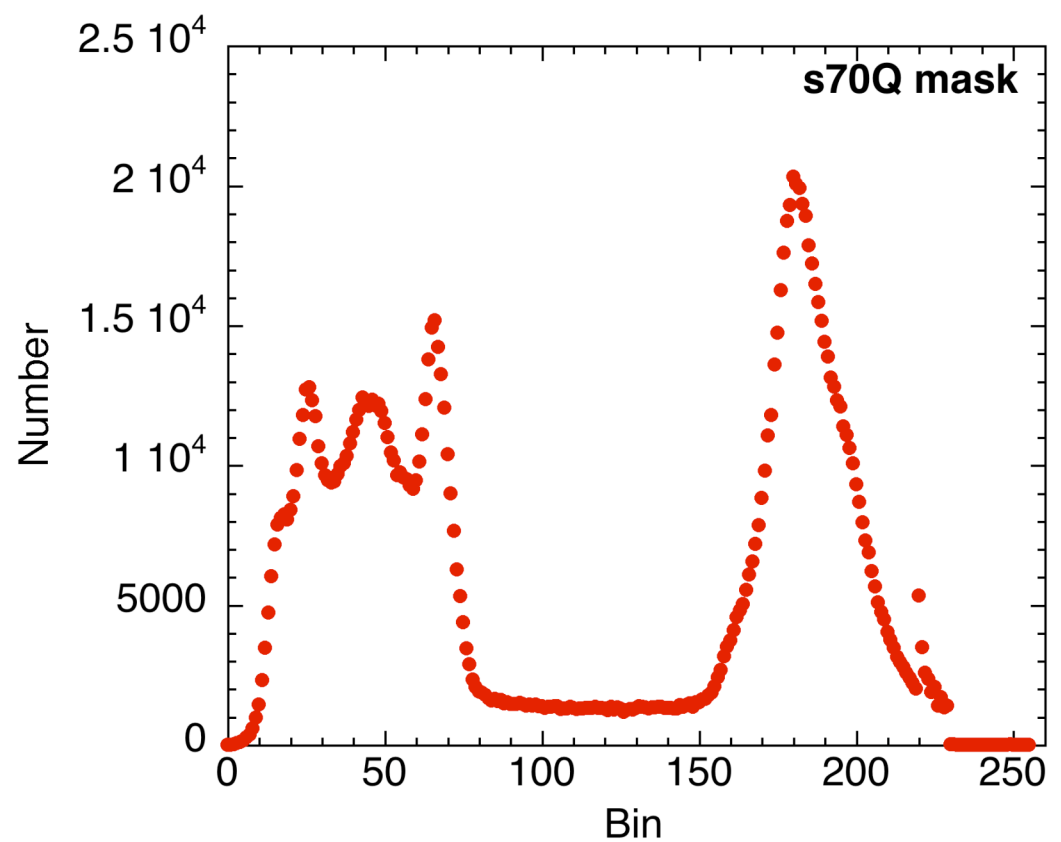
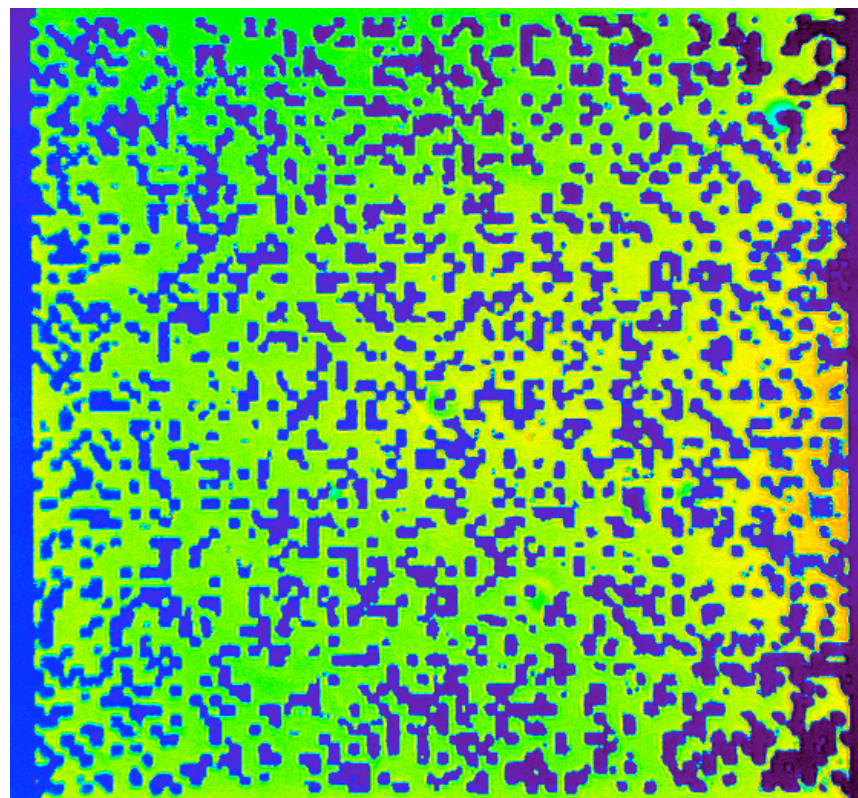
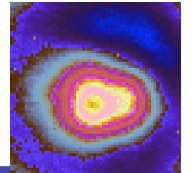
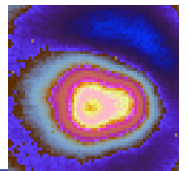


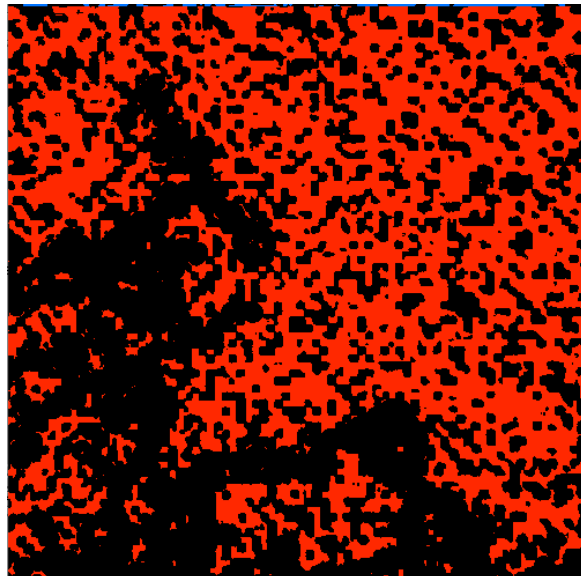
Image Analysis: Threshold



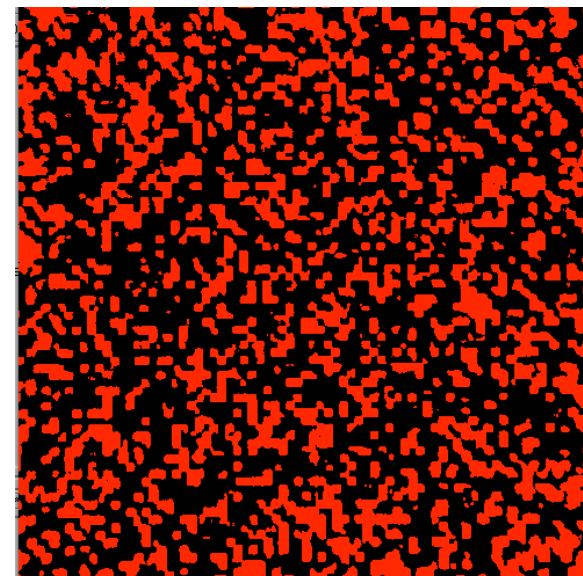


Phase Identification

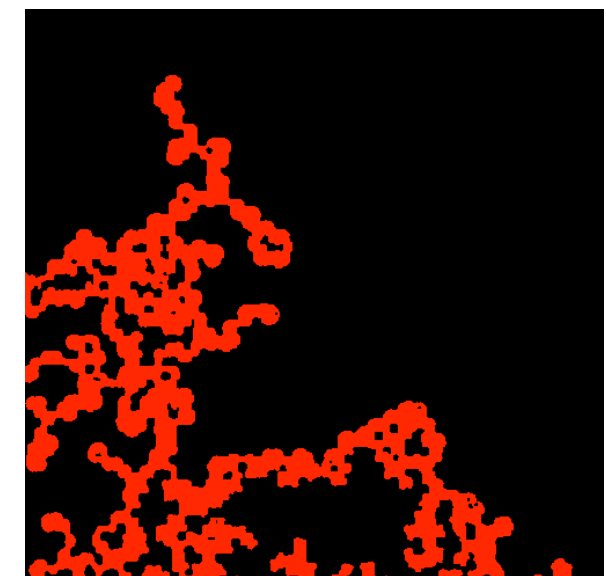
Decane



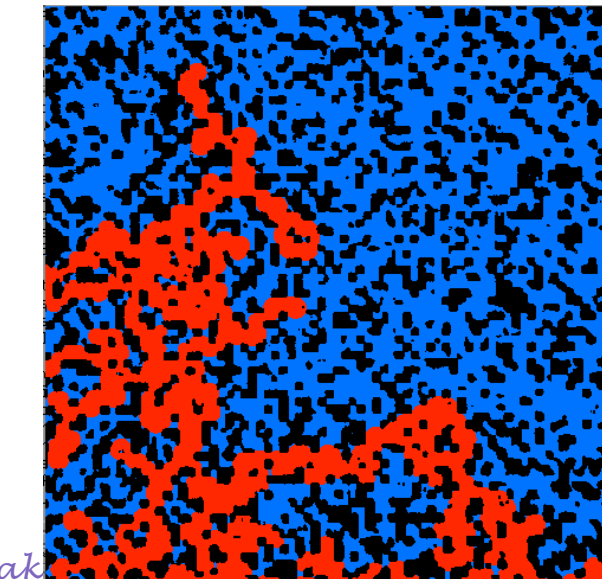
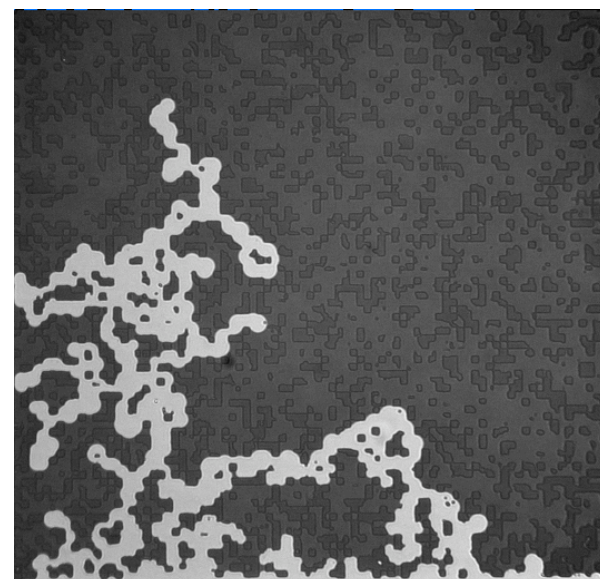
Photoresist



Nitrogen

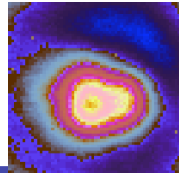


Raw
Image



False
Color
Image

Image Analysis



From Image Analysis:

- ❖ Saturation
- ❖ Interfacial Length
- ❖ Curvature
- ❖ Normals to Interfaces

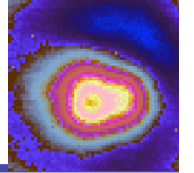


Image Analysis: Convolution Kernels

Image									
I ₁₁	I ₁₂	I ₁₃	I ₁₄	I ₁₅	I ₁₆	I ₁₇	I ₁₈	I ₁₉	
I ₂₁	I ₂₂	I ₂₃	I ₂₄	I ₂₅	I ₂₆	I ₂₇	I ₂₈	I ₂₉	
I ₃₁	I ₃₂	I ₃₃	I ₃₄	I ₃₅	I ₃₆	I ₃₇	I ₃₈	I ₃₉	
I ₄₁	I ₄₂	I ₄₃	I ₄₄	I ₄₅	I ₄₆	I ₄₇	I ₄₈	I ₄₉	
I ₅₁	I ₅₂	I ₅₃	I ₅₄	I ₅₅	I ₅₆	I ₅₇	I ₅₈	I ₅₉	
I ₆₁	I ₆₂	I ₆₃	I ₆₄	I ₆₅	I ₆₆	I ₆₇	I ₆₈	I ₆₉	

Kernel

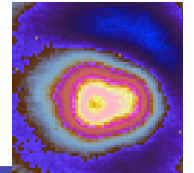
K ₁₁	K ₁₂	K ₁₃
K ₂₁	K ₂₃	K ₃₃

<http://homepages.inf.ed.ac.uk/rbf/HIPR2/convolve.htm>

$$O(i, j) = \sum_{k=1}^m \sum_{l=1}^n I(i+k-1, j+l-1)K(k, l)$$

$$O_{57} = I_{57}K_{11} + I_{58}K_{12} + I_{59}K_{13} + I_{67}K_{21} + I_{68}K_{22} + I_{69}K_{23}$$

Edge Detection



Sobel

-1	0	+1
-2	0	+2
-1	0	+1

Gx

+1	+2	+1
0	0	0
-1	-2	-1

Gy

Roberts

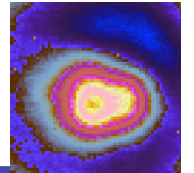
+1	0
0	-1

Gx

0	+1
-1	0

Gy

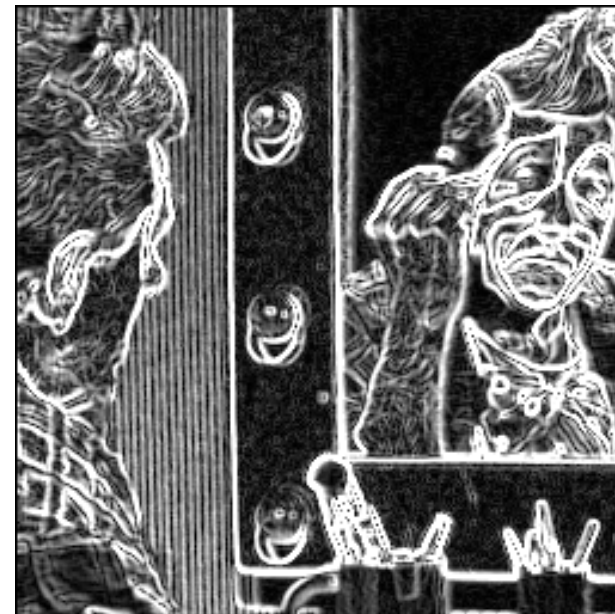
Edge Detection



Image



Sobel

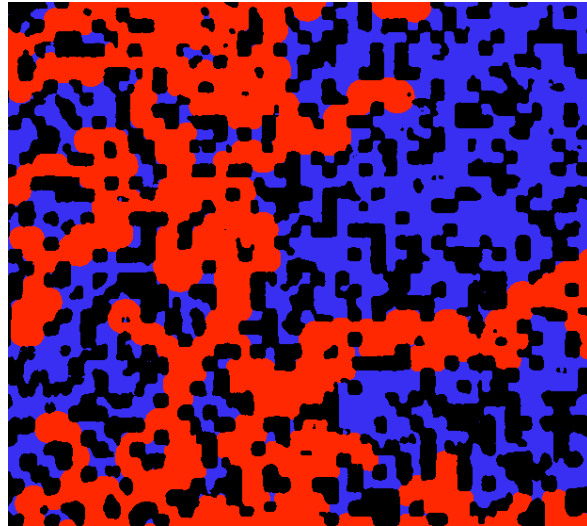
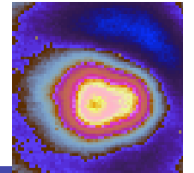


Roberts

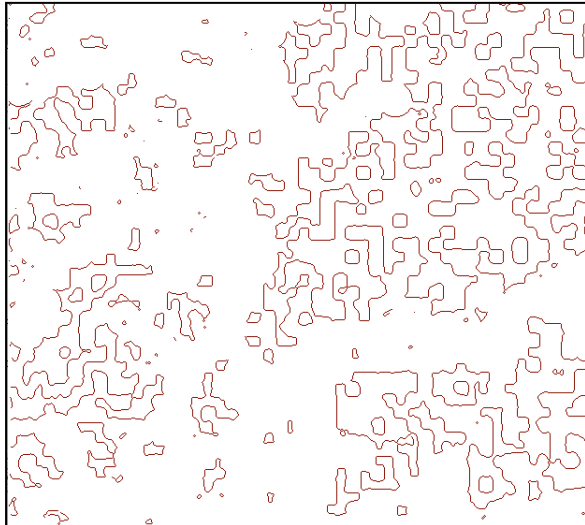


<http://homepages.inf.ed.ac.uk/rbf/HIPR2/sobel.htm>

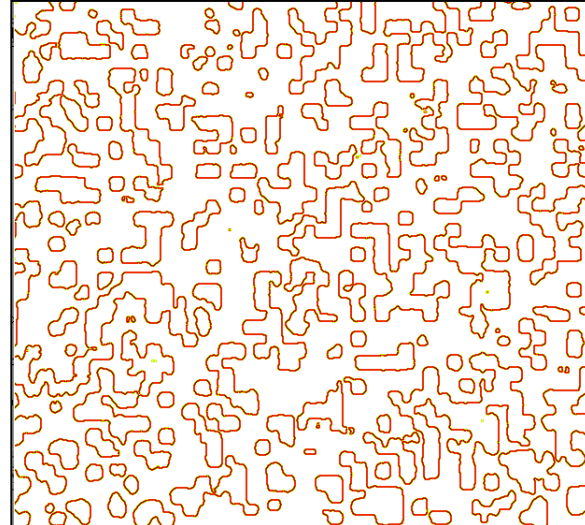
Image Analysis: Edge Detection



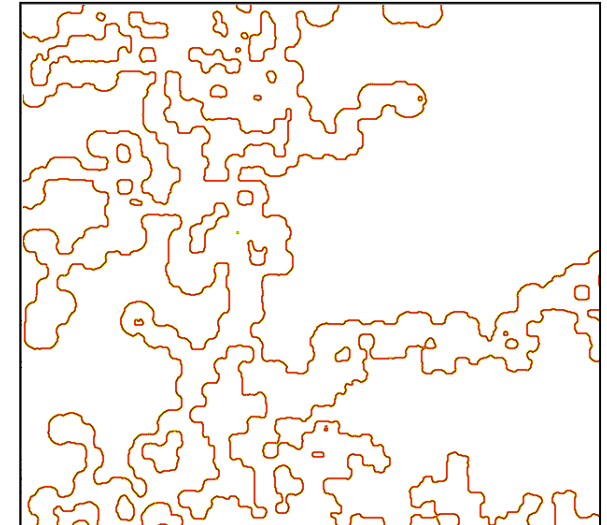
Decane Interfaces



Photoresist Interfaces



Nitrogen Interfaces



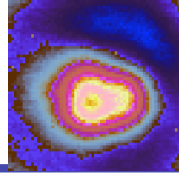
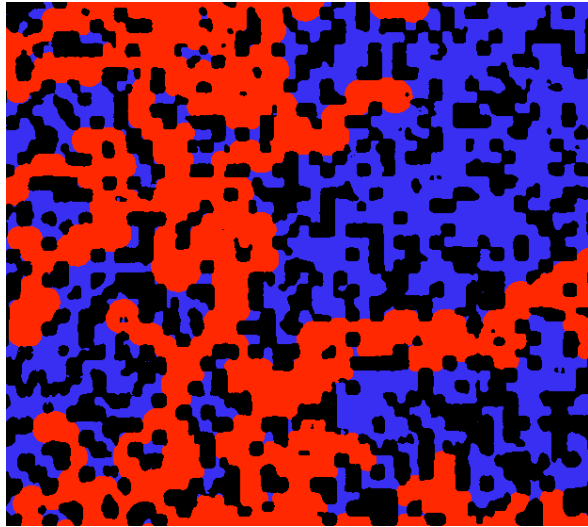


Image Analysis: Interfaces



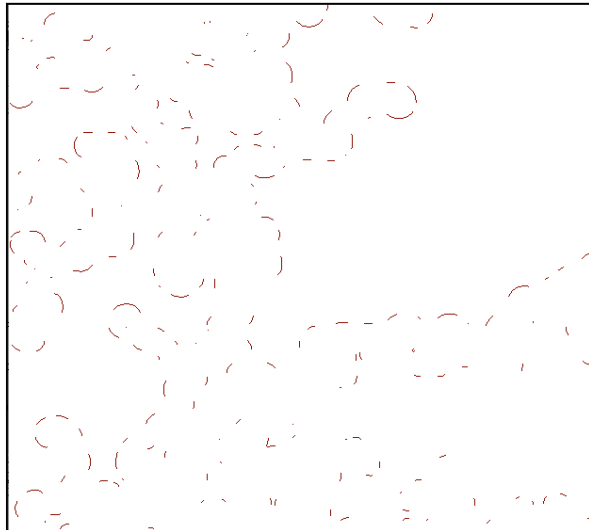
Interfacial Length

$$L_{wn} = (L_n + L_w - L_s) / 2$$

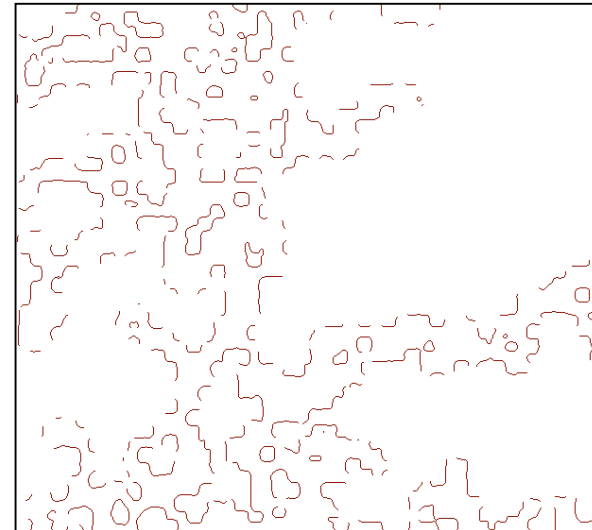
$$L_{ns} = (L_n + L_s - L_w) / 2$$

$$L_{ws} = (L_w + L_s - L_n) / 2$$

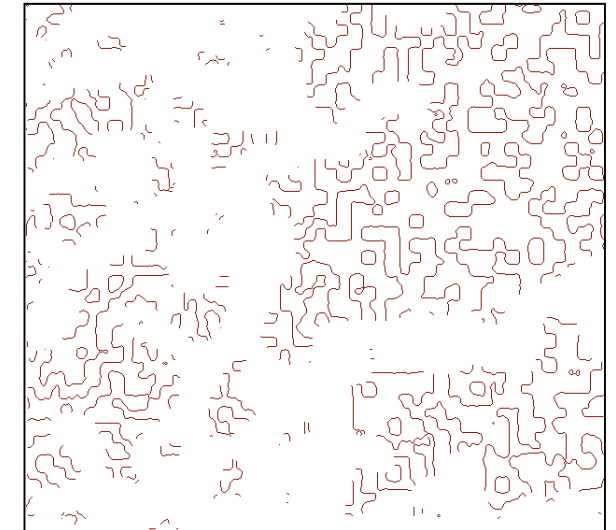
wn interfaces



ns interfaces

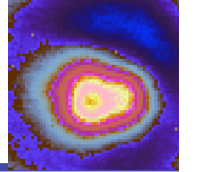


ws interfaces



Pyrak-Nolte

08



Curvature: Kernel Approach

$$K = \frac{\Phi_y^2 \Phi_{xx} - 2\Phi_x \Phi_y \Phi_{xy} + \Phi_x^2 \Phi_{yy}}{(\Phi_x^2 + \Phi_y^2)^{3/2}}$$

$$\Phi_x = [-0.5, 0, 0.5]$$

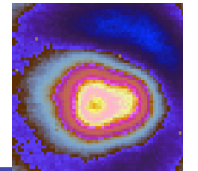
$$\Phi_y = \text{transpose}[\Phi_x]$$

$$\Phi_{xx} = [1.0, -2.0, 1.0]$$

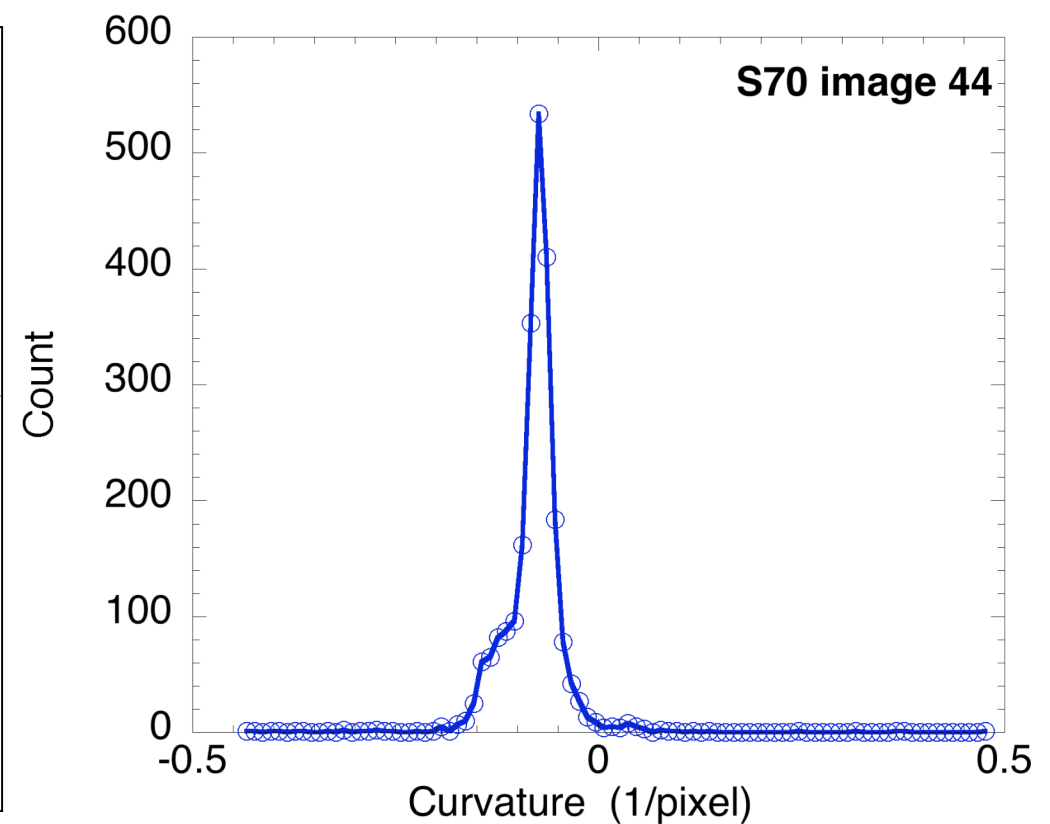
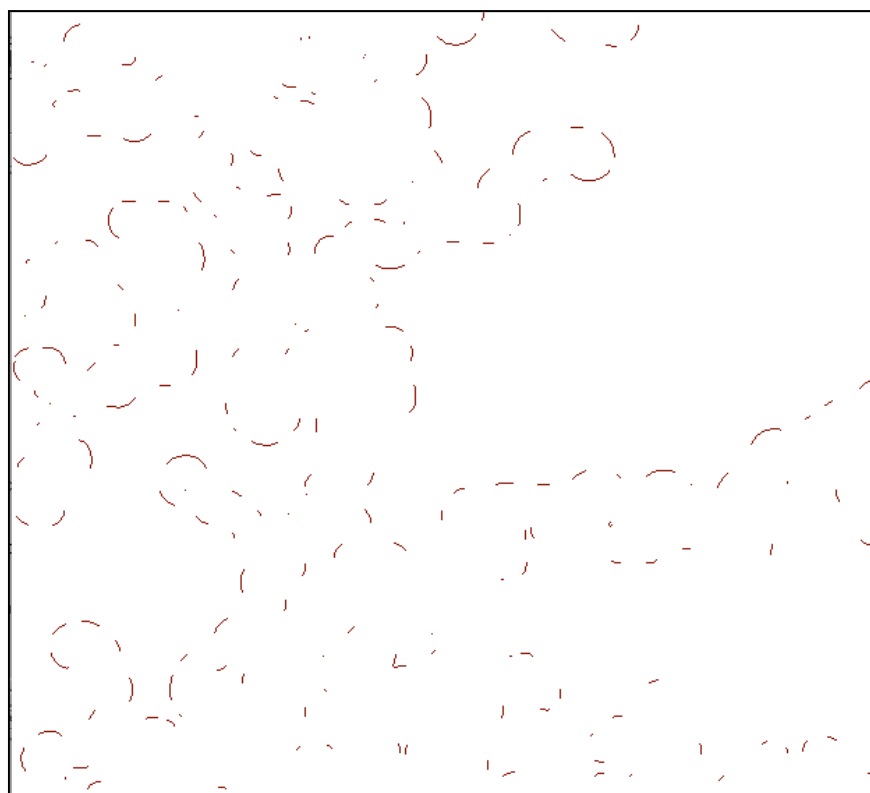
$$\Phi_{yy} = \text{transpose}[\Phi_{xx}]$$

$$\Phi_{xy} = \begin{bmatrix} 0.25 & 0 & -0.25 \\ 0 & 0 & 0 \\ 0.25 & 0 & -0.25 \end{bmatrix}$$

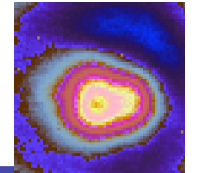
Curvature of wn Interfaces



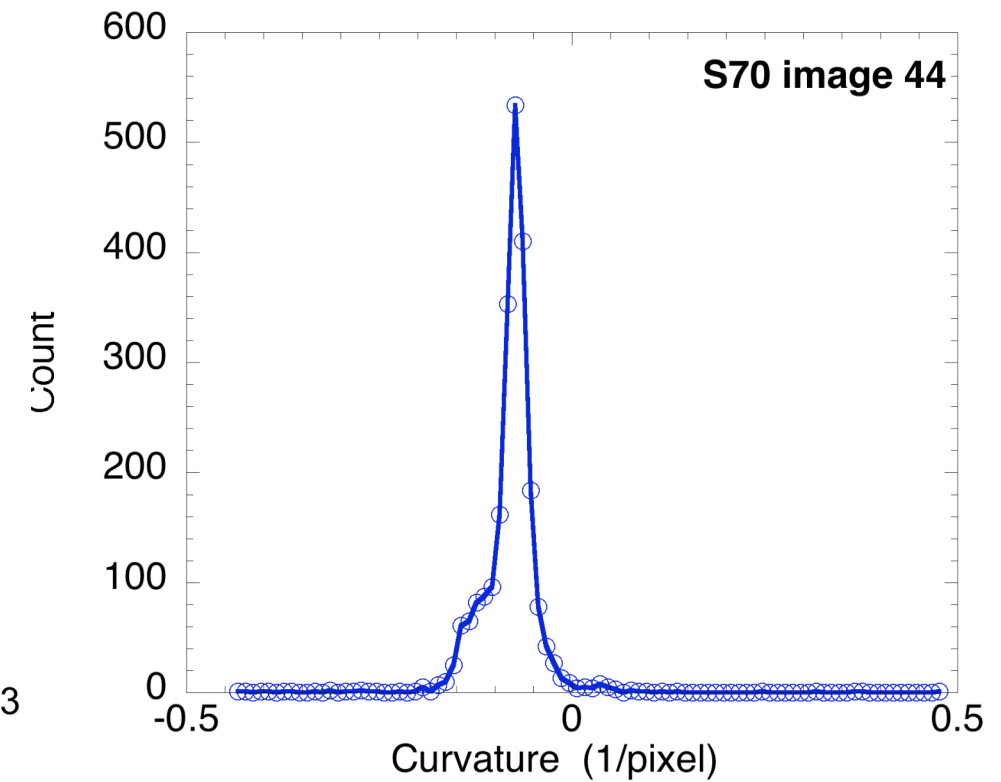
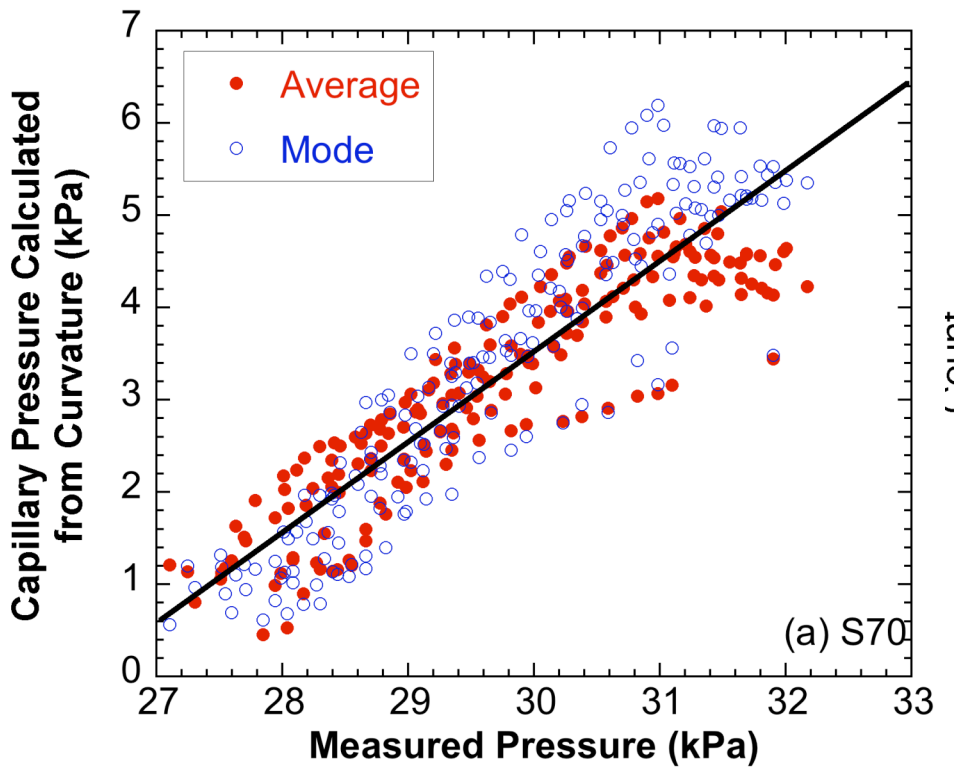
wn interfaces

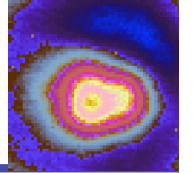


Mode versus Average



wn interfaces





Normals

$$n_x = \frac{\Phi_x}{\sqrt{\Phi_x^2 + \Phi_y^2}}$$

$$n_y = \frac{\Phi_y}{\sqrt{\Phi_x^2 + \Phi_y^2}}$$

$$n_{xx} = \text{Image} * n_x n_x$$

$$n_{yy} = \text{Image} * n_y n_y$$

$$n_{xy} = \text{Image} * n_x n_y$$

Thank you!

